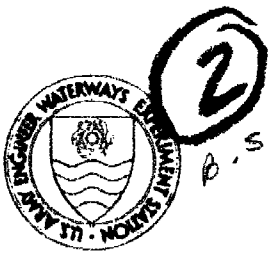

TECHNICAL REPORT S-77-4

INVESTIGATION OF A PROPOSED FULL-SCALE ROCK PENETRATION TEST SITE NEAR LOS LUNAS, NEW MEXICO

by

Dwain K. Butler

Soils and Pavements Laboratory
U. S. Army Engineer Waterways Experiment Station
P. O. Box 631, Vicksburg, Miss. 39180

May 1977
Final Report

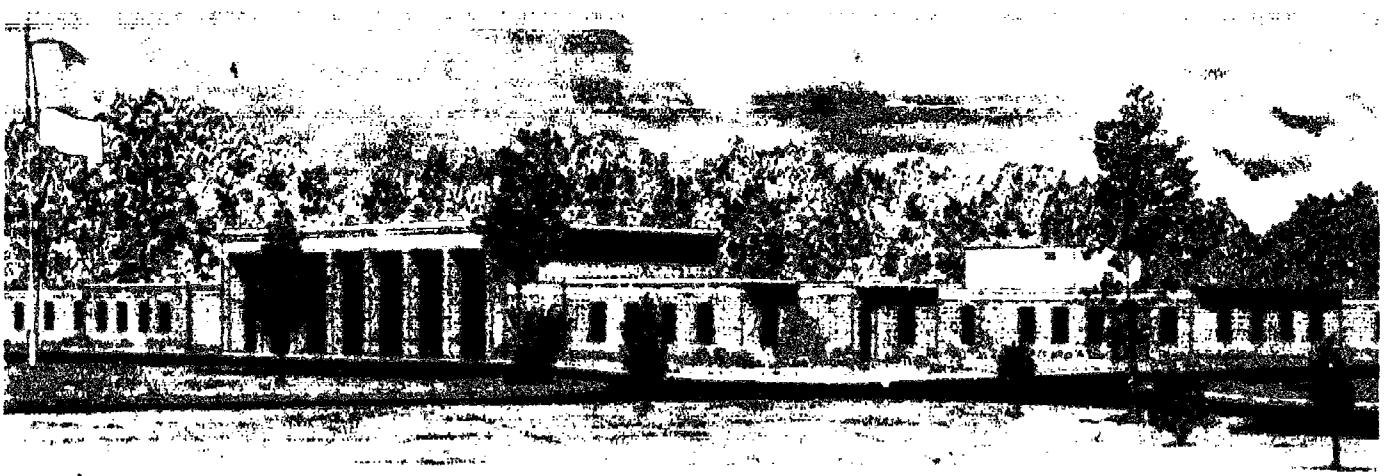

Prepared for Defense Nuclear Agency
Washington, D. C. 20305

Under Subtask SB211, Work Unit 11, "Field Firing Material Testing"

Destroy this report when no longer needed. Do not return it to the originator.

Unclassified

SECURITY CLASSIFICATION OF THIS PAGE (When Data Entered)

REPORT DOCUMENTATION PAGE

READ INSTRUCTIONS BEFORE COMPLETING FORM

1. REPORT NUMBER: Technical Report S-77-4	2. GOVT ACCESSION NO.
3. RECIPIENT'S CATALOG NUMBER	
4. TITLE (and Subtitle): INVESTIGATION OF A PROPOSED FULL-SCALE ROCK PENETRATION TEST SITE NEAR LOS LUNAS, NEW MEXICO	5. TYPE OF REPORT & PERIOD COVERED: Final report. Jul-Oct 76
	6. PERFORMING ORG. REPORT NUMBER
7. AUTHOR(s): Dwain K. Butler	8. CONTRACT OR GRANT NUMBER(s)
9. PERFORMING ORGANIZATION NAME AND ADDRESS: U. S. Army Engineer Waterways Experiment Station, Soils and Pavements Laboratory, P. O. Box 631, Vicksburg, Miss. 39180	10. PROGRAM ELEMENT, PROJECT, TASK AREA & WORK UNIT NUMBERS: Subtask SB211, Work Unit 11
11. CONTROLLING OFFICE NAME AND ADDRESS: Defense Nuclear Agency, Washington, D. C. 20305	12. REPORT DATE: May 1977
	13. NUMBER OF PAGES: 12 152 p.
14. MONITORING AGENCY NAME & ADDRESS (if different from Controlling Office)	15. SECURITY CLASS. (of this report): Unclassified
	15a. DECLASSIFICATION/DOWNGRADING SCHEDULE

16. DISTRIBUTION STATEMENT (of this Report)

Approved for public release; distribution unlimited.

17. DISTRIBUTION STATEMENT (of the abstract entered in Block 20, if different from Report)

18. SUPPLEMENTARY NOTES

This work was sponsored by the Defense Nuclear Agency under Subtask SB211, Work Unit 11, "Field Firing Material Testing."

19. KEY WORDS (Continue on reverse side if necessary and identify by block number)

Los Lunas, N. Mex.
Penetration
Rock masses
Rock tests (laboratory)
Site investigation

20. ABSTRACT (Continue on reverse side if necessary and identify by block number)

Results of a field investigation at a proposed DNA full-scale rock penetration site near Los Lunas, New Mexico, and of classification, composition, and mechanical property tests on rock from the site are presented. The mechanical property tests were conducted on material from the upper 3 metres of the site, where the rock is a fine- to medium-grain, red, arkosic sandstone member of the Yeso Formation. This site was intended to be the very-low-strength member of a set of three test sites in medium-, low-, and

(Continued)

DD FORM 1 JAN 73 1473 EDITION OF 1 NOV 65 IS OBSOLETE

Unclassified

SECURITY CLASSIFICATION OF THIS PAGE (When Data Entered)

20. ABSTRACT (Continued).

very-low-strength rock. As a result of the strength data from the laboratory test program, however, it became apparent that the overall program objectives would not be achieved with the Los Lunas site, since (1) the near-surface strength is intermediate between those at two sites already used for full-scale penetration tests, and (2) a layer interface exists (below which lies an even higher strength rock) at the site within the depth range which would be exercised in a penetration test (3 to 5 metres). Consequently, it was recommended to DNA that the remaining full-scale penetration test not be conducted at the Los Lunas site.

PREFACE

This investigation was conducted during the period July 1976 - October 1976 by personnel of the Soil Dynamics Division (SDD) of the Soils and Pavements Laboratory (S&PL), U. S. Army Engineer Waterways Experiment Station (WES). The work was sponsored by the Defense Nuclear Agency (DNA) under Subtask SB211, Work Unit 11, "Field Firing Material Testing."

The investigation was planned and conducted by Mr. D. K. Butler, SDD. Technical consultation and guidance were provided by Dr. P. F. Hadala, SDD. Mr. J. R. Curro of the Earthquake Engineering and Vibrations Division, WES, conducted the field geophysical survey. The work was performed under the general supervision of Dr. J. G. Jackson, Jr., Chief, SDD, and Mr. J. P. Sale, Chief, S&PL.

COL G. H. Hilt, CE, and COL J. L. Cannon, CE, were Directors of WES and Mr. F. R. Brown was Technical Director during this period.

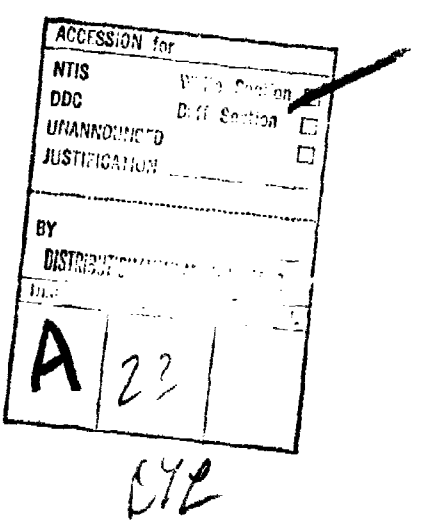

CONTENTS

CHAPTER 1

INTRODUCTION

1.1 BACKGROUND

The full-scale penetration tests being conducted as part of the Defense Nuclear Agency's (DNA) Earth Penetration Weapon (EPW) Research Program are concerned with assessing the survivability of candidate EPW's following impact and the penetrability of hard targets. Three rock types were initially selected for the targets: welded tuff, sandstone, and shale. These types of rock were selected since presumably they would cover a wide range of strength ("hardness" or resistance to penetration) and could qualitatively be described as being medium-, low-, and very-low-strength targets, respectively.

The first test site selected was a welded tuff site, located near Mount Helen on the Tonopah Test Range (TTR), Nevada. Reference 1 presents the results of field investigations and laboratory constitutive property tests on rock from the site. With an average unconfined compressive strength of 0.64 kbar (9300 psi) for the first 3 metres depth, the welded tuff meets the qualitative criterion for a medium-strength rock target. Five penetration tests were conducted at the TTR site during the period of July 1975 to April 1976 by Sandia Laboratories, Albuquerque (SLA).[2]

The second site, a sandstone site, is located near San Ysidro, New Mexico. The Dakota sandstone target material at this site has an average unconfined compressive strength of 0.23 kbar (3300 psi) for the first 3 metres depth, meeting the qualitative criterion for a low-strength rock. Results of field and laboratory investigations for this site are presented in Reference 3. Two penetration tests were conducted at the site in July 1976 by SLA. Large blocks of sandstone from this site have been used in DNA-sponsored reverse ballistic tests conducted by Avco Corporation in August 1976.

A shale site (for the very-low-strength target) which was accessible by the heavy equipment required for field penetration tests, met the test

safety requirements, and was within reasonable distance of SLA's base of operations could not be located. Subsequently, a siltstone site was located near Los Lunas, New Mexico, which was considered satisfactory for use for field penetration tests.[4] It was hoped that this might replace the shale site. Results of laboratory testing presented in this report reveal, however, that the average unconfined compressive strength of the first 3 metres depth of this site is 0.46 kbar (6700 psi); and, at greater depths, the strength of the massive siltstone exceeds the strength of the TTR welded tuff. Hence, penetration tests at the Los Lunas siltstone site would not fulfill the original field test program objectives and it was decided by DNA, on the basis of the test data reported herein, to delete the third site from the program.

1.2 PURPOSE

The purposes of this report are to present for the record (1) the results of a field investigation at the proposed penetration test site near Los Lunas, New Mexico, and (2) the results of laboratory tests on rock core from the site. The field drilling and sampling program and geophysical survey are discussed in Chapter 2. Results of laboratory composition tests and mechanical property tests are presented in Chapter 3; and, finally, a summary of the test results and a description of the events leading to the decision not to use this site for full-scale penetration tests are presented in Chapter 4.

CHAPTER 2

SITE INVESTIGATIONS AND RESULTS

2.1 SITE DESCRIPTION

The proposed penetration site is located about 70 kilometres southwest of Albuquerque, New Mexico, and about 35 kilometres west of Los Lunas, New Mexico. Figure 2.1 presents regional and local site location maps. The site is at 1800 metres elevation near the base of a large mesa, and is not easily accessible. There are no close habitations, but considerable airplane traffic can be heard.

Surface rock at the site chosen for drilling is a fine- to medium-grained red sandstone member of the Yeso Formation of Permian age. The sandstone overlies the siltstone which is exposed at one of the three nearby but less accessible sites originally selected. Beds dip 5 to 10 degrees to the north, which is also the surface slope. There are two rock terraces at the site with an elevation difference of 3 to 4 metres. The upper terrace is about 12 metres by 50 metres in size, and the lower terrace has about 15 metres by 100 metres of completely exposed and accessible rock surface. Due to its larger size and the absence of fractures in the central portion, the lower terrace was deemed the better for a penetration test location and was chosen for the drilling program.

Figure 2.2 is the site boring layout and shows the locations of the only observable vertical fractures in the region of interest on the lower terrace. The two open fractures are filled with sand. Horizontal fractures are observable in the sandstone on exposed vertical faces, with a nominal 5-centimetre spacing. Near boreholes NX-1 and NX-3 the rock "sounds hollow" when struck. This is apparently due to near-surface weathering along what may be release fractures or bedding planes. In any event, the weathered zone which is generally friable appears to extend only to a depth of about 50 centimetres. Below this depth the material exposed on vertical faces is hard and massive. Also

visible on these faces, as well as on portions of the surface, are small, irregular regions of light tan to white sandstone. The difference between the red and light tan sandstone is apparently the absence of iron oxide in the light tan areas.

2.2 FIELD DRILLING AND SAMPLING PROGRAM

The field drilling and sampling program was designed to obtain samples of rock from the site to support laboratory testing programs.* Two 9-metre-deep (NX-1 and NX-2) and one 6-metre-deep (NX-3) NX-diameter (5.4-centimetre-diameter) holes were drilled using air and diamond core bits during July 1976. The core samples were logged, RQD was determined, and samples were waxed to preserve water content. Also, a 12.7-centimetre-diameter hole (U-1) was drilled 4.5 metres deep using a modified Dennison sampler. This device retains the cores in steel tubes which are then sealed by O-ring packers at the ends. The site boring layout is shown in Figure 2.2.

Logs and pertinent comments for the three NX holes are presented in Figure 2.3. The medium-grained red sandstone is encountered to depths of 3 to 4 metres in all three holes, where a transition to a red, hard, dense siltstone occurs. Except for the upper metre of the holes, the rock quality is very high (i.e., few fractures, RQD ≈ 100 percent).

2.3 GEOPHYSICAL SURVEY

The geophysical survey at the site was designed to determine the in situ compression- and shear-wave (P- and S-wave) velocities and depths to seismic interfaces from the surface to a depth of at least 9 metres. Included in the survey, which was conducted in July 1976,

---

* In addition to this program, which evaluated the suitability of the site, sufficient samples were taken to support extensive high-pressure static and dynamic constitutive property tests which would have been conducted if the site had proved acceptable.

were surface seismic refraction traverses, a surface S-wave test, downhole P- and S-wave tests, and crosshole P- and S-wave tests. A detailed description of these tests (equipment and test procedures) is given in Reference 3. Figure 2.4 is a plan view of the site showing the geophysical test locations.

Two reverse-traverse, surface seismic refraction tests were conducted. As shown in Figure 2.4, the hammer impulse location for traverse S-1 was beside borehole NX-1 and the direction of S-1 was the same as the direction from borehole NX-1 to borehole NX-2. Traverses S-3 and S-4 were located on the upper terrace. Results of the surface refraction tests are given in Figures 2.5-2.8. The results of both sets of traverses show two P-wave velocity layers. Note that the depth to the interface (see Figure 2.8) under the upper terrace corresponds to the elevation difference between the upper and lower terrace and that the second-layer velocity for the upper terrace corresponds to the first-layer velocity for the lower terrace. The surface S-wave test arrival time versus distance plot is presented in Figure 2.9. The test location is shown in Figure 2.4.

Average and incremental P- and S-wave velocities from the downhole tests in boreholes NX-2 and NX-3 are presented in Figures 2.10 and 2.11, respectively. Finally, the results of the crosshole P- and S-wave tests are shown in Figures 2.12-2.15. Also, Figures 2.12-2.15 illustrate the P- and S-wave velocity profiles interpreted from the surface data and the downhole and crosshole data. Note that the interpreted velocity interface agrees quite well with the interface between the medium-grained red sandstone and the red siltstone (see Figure 2.3).

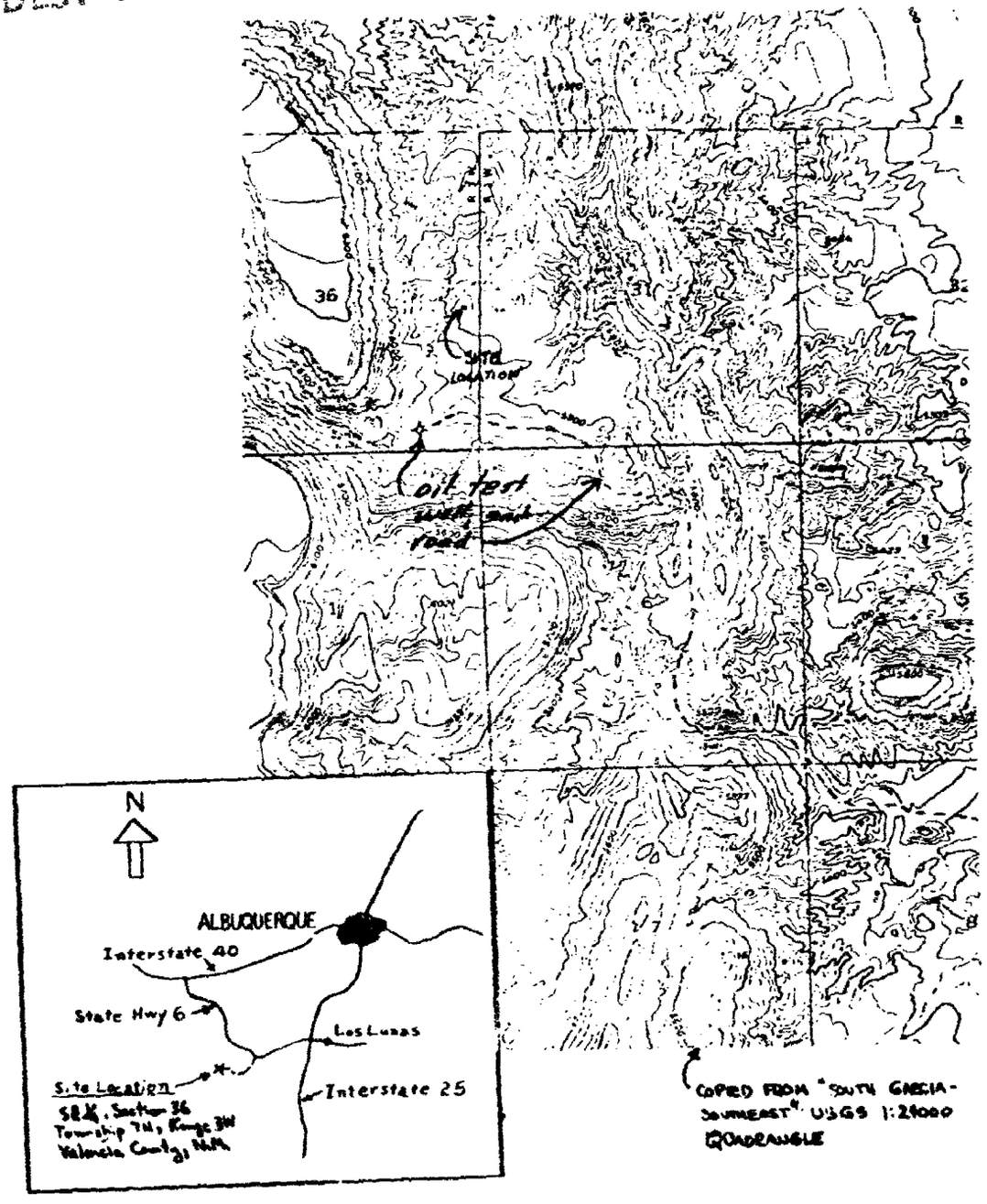

Figure 2.1. Site location map.

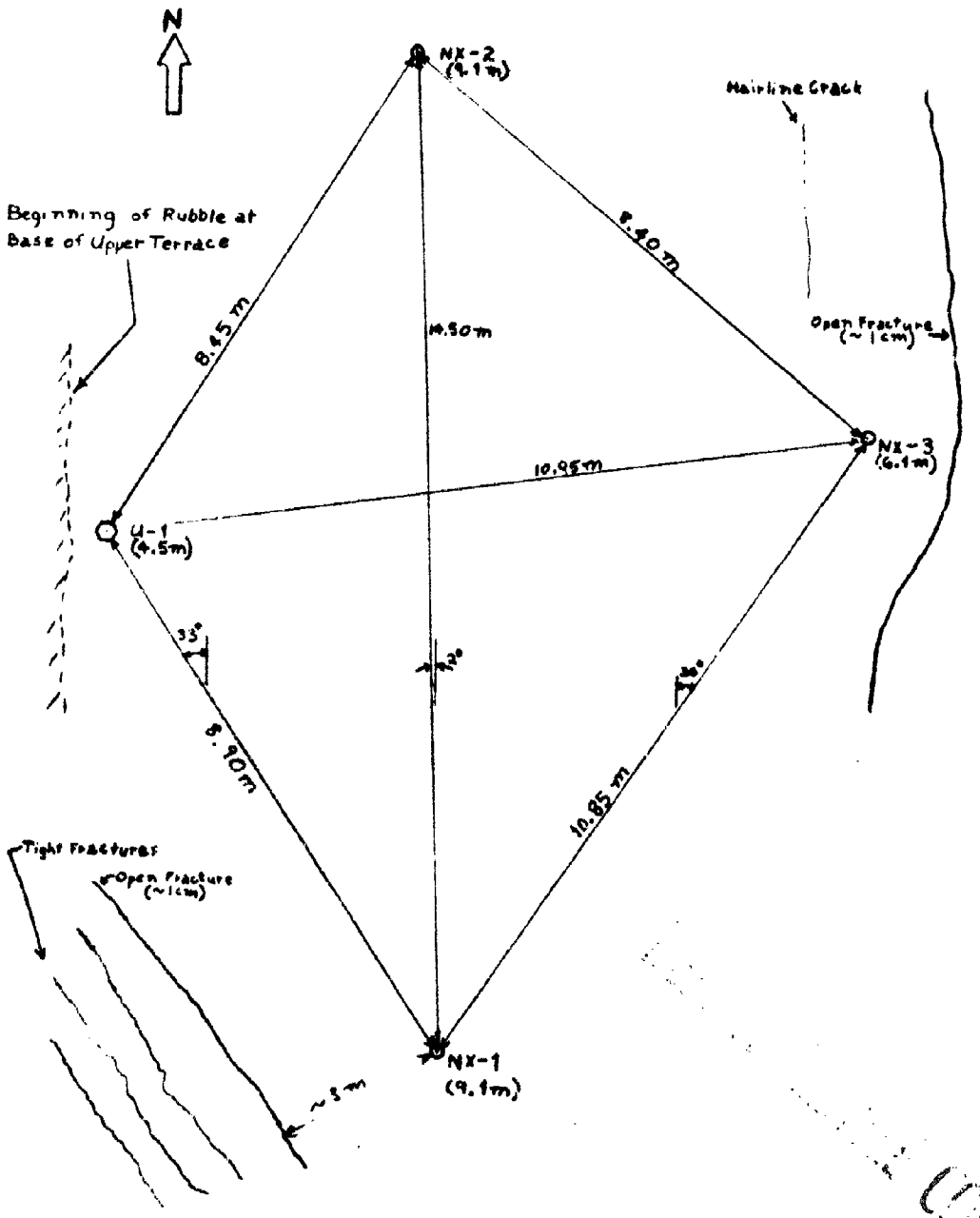

Figure 2.2. Site boring layout.

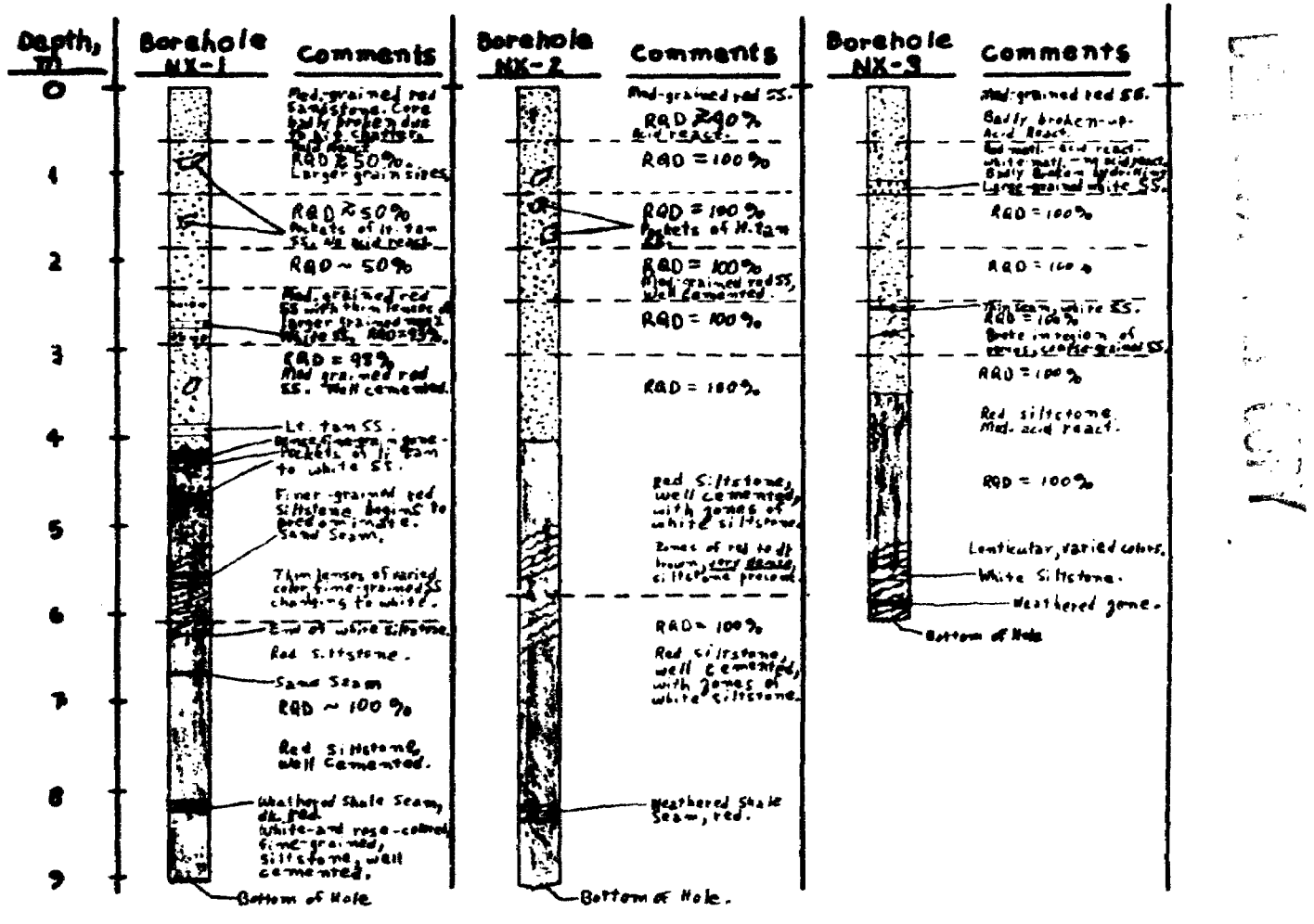

Figure 2.3. Boring logs for NX holes at Los Lunas site.

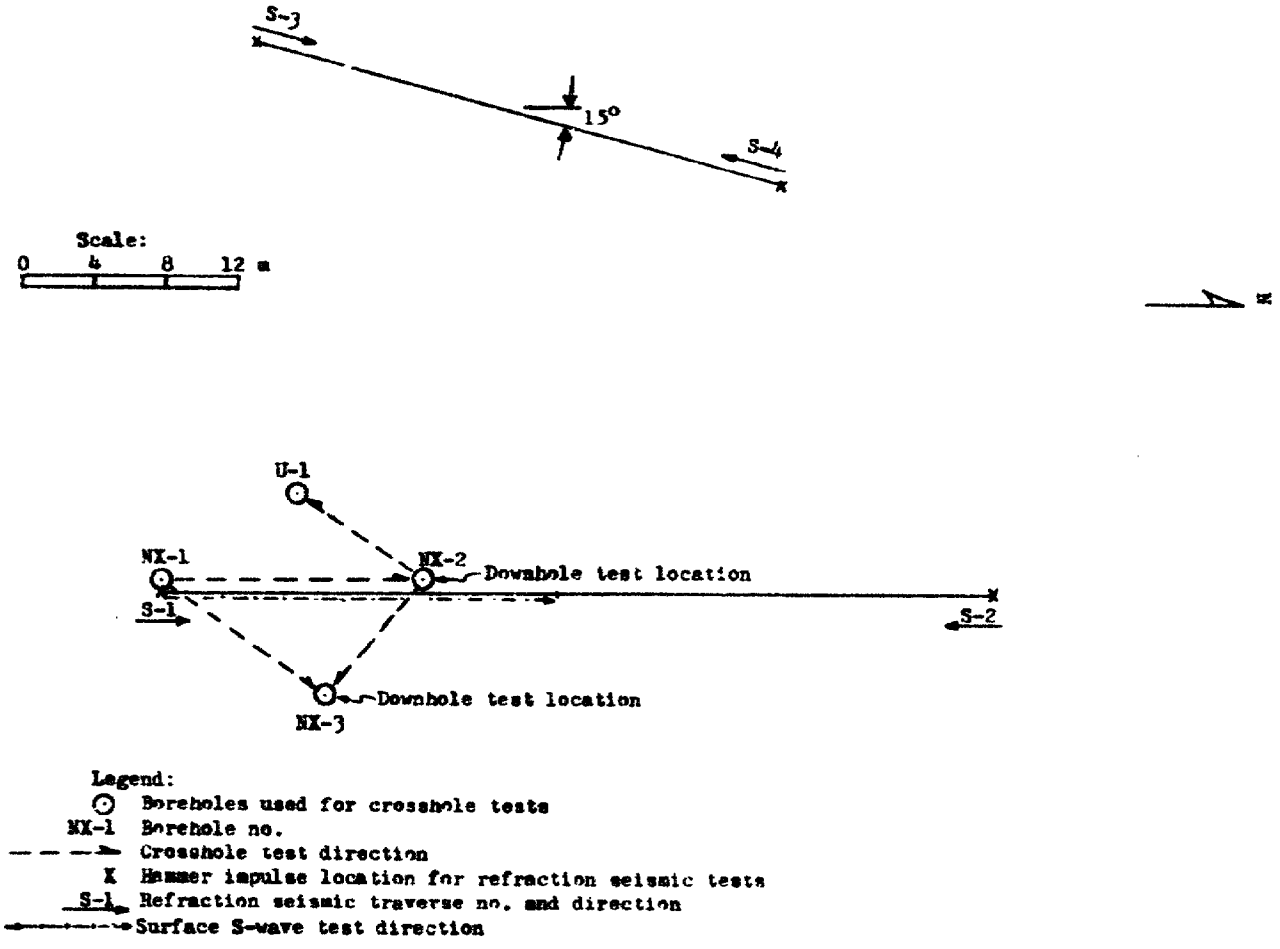

Figure 2.4. Plan view showing crosshole, downhole, surface S-wave, and refraction seismic test layouts.

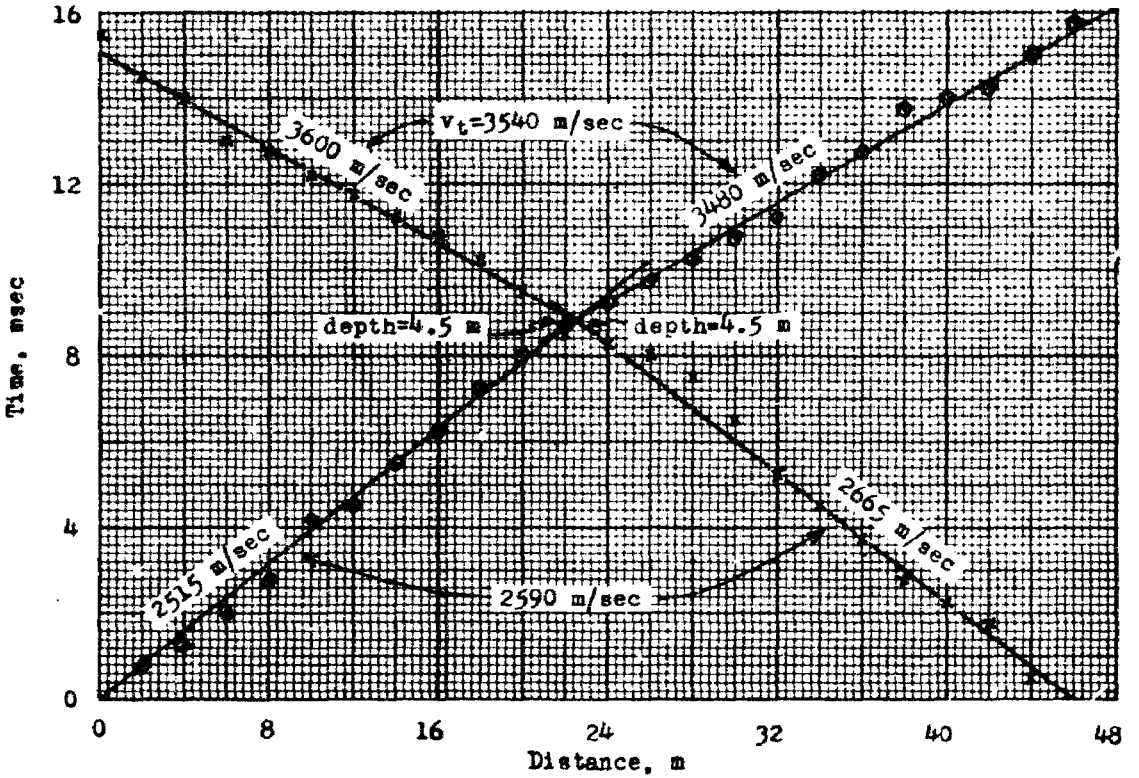

Figure 2.5. P-wave arrival time versus distance from surface refraction seismic traverses S-1 and S-2.

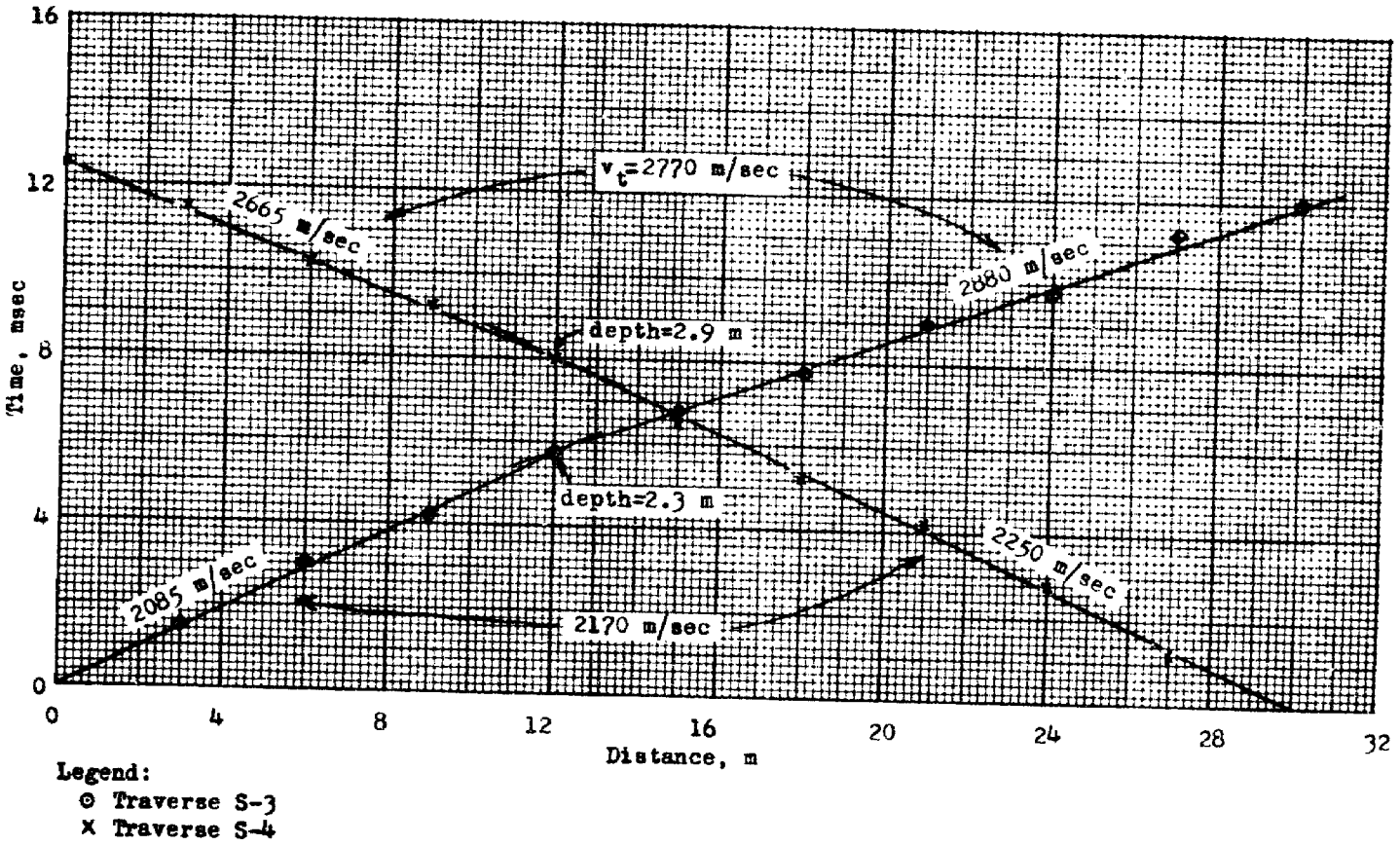

Figure 2.6. P-wave arrival time versus distance from surface refraction seismic traverses S-3 and S-4.

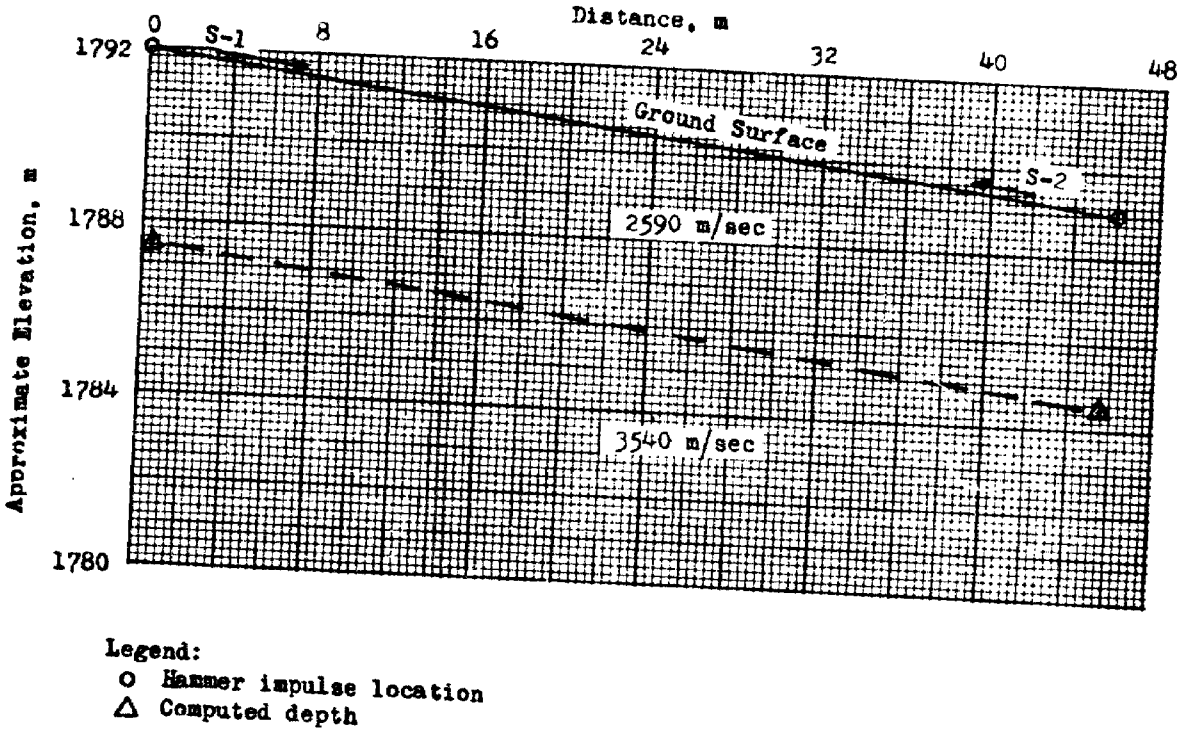

Figure 2.7. Approximate P-wave velocity profile determined from surface refraction seismic traverses S-1 and S-2.

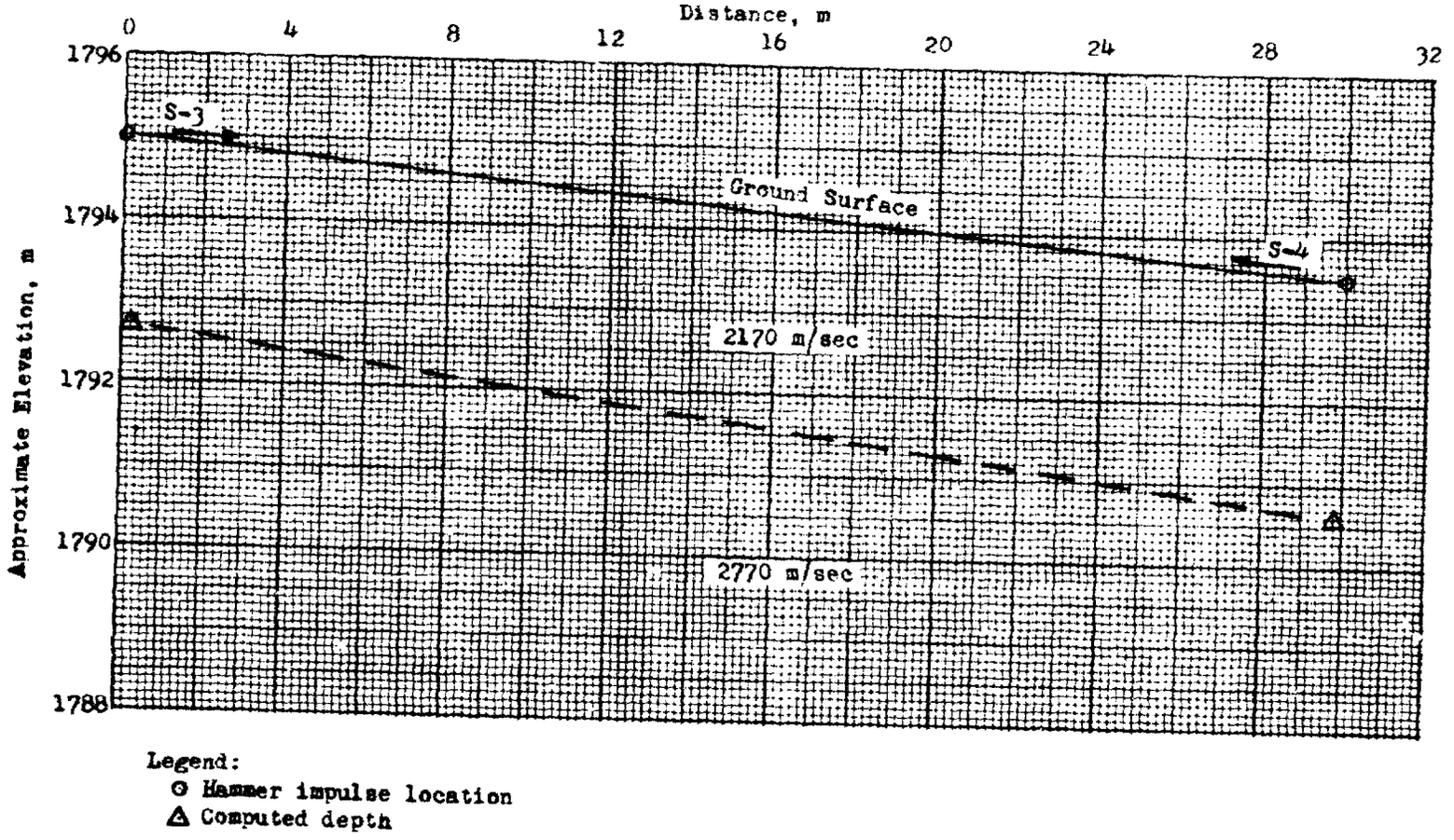

Figure 2.8. Approximate P-wave velocity profile determined from surface refraction seismic traverses S-3 and S-4.

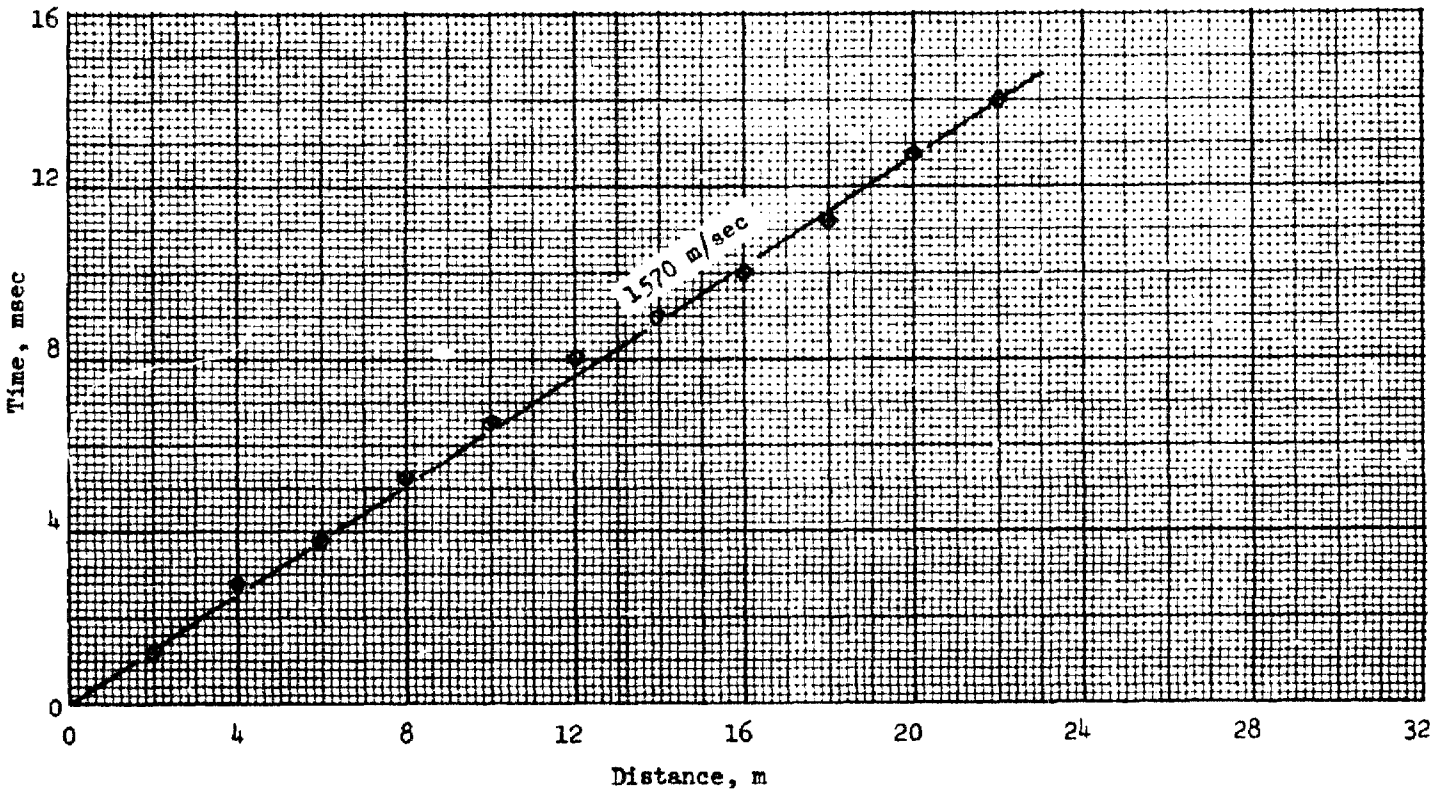

Figure 2.9. S-wave arrival time versus distance from surface S-wave test.

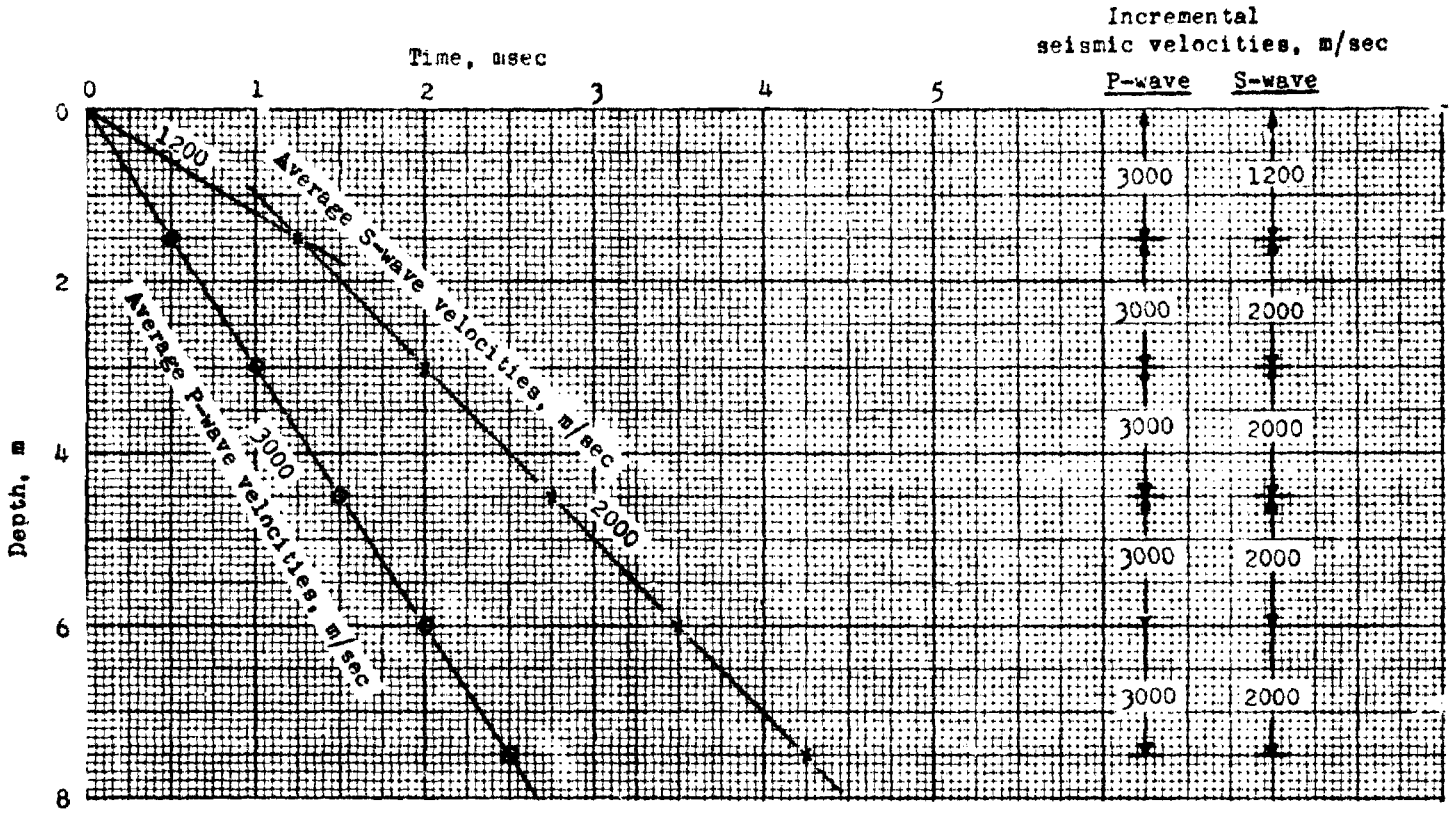

Figure 2.10. P- and S-wave arrival time versus depth from downhole test conducted in boring NX-2.

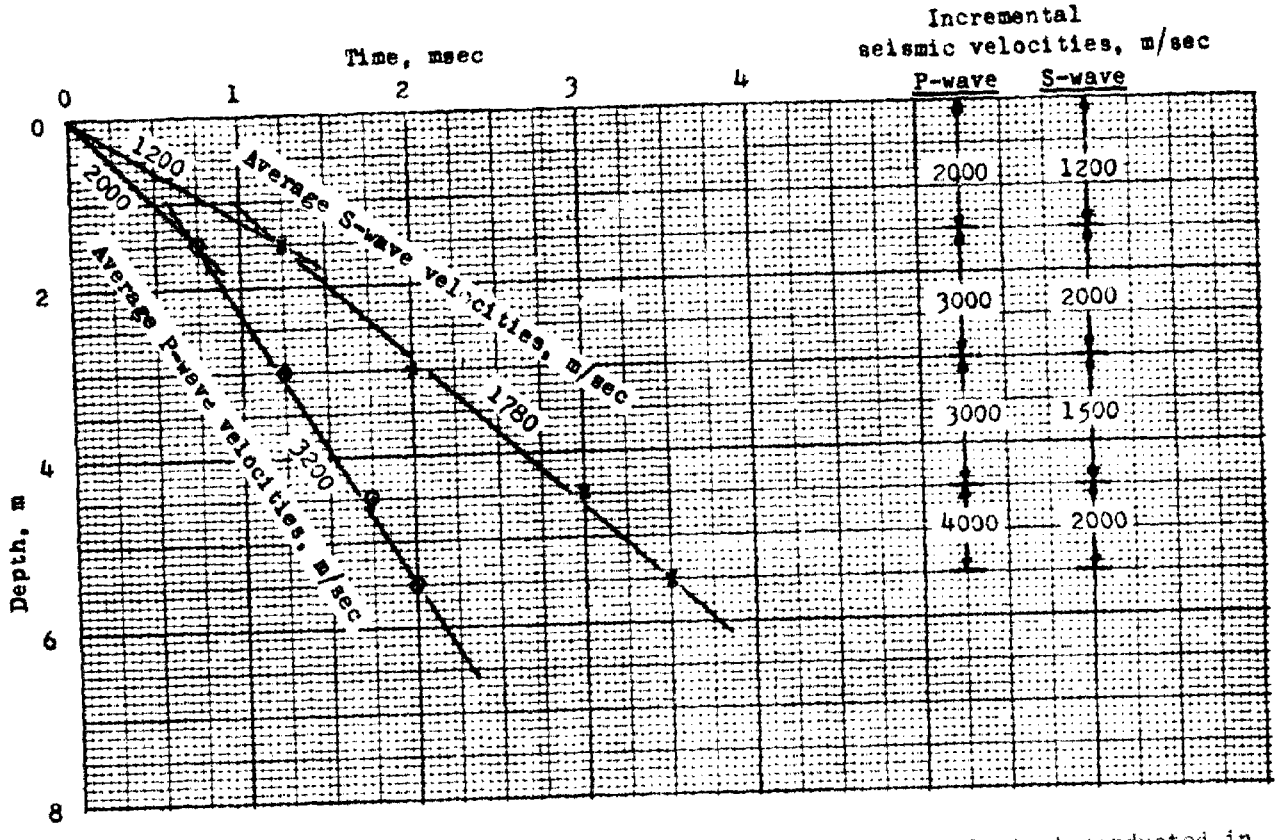

Figure 2.11. P- and S-wave arrival time versus depth from downhole test conducted in boring NX-3.

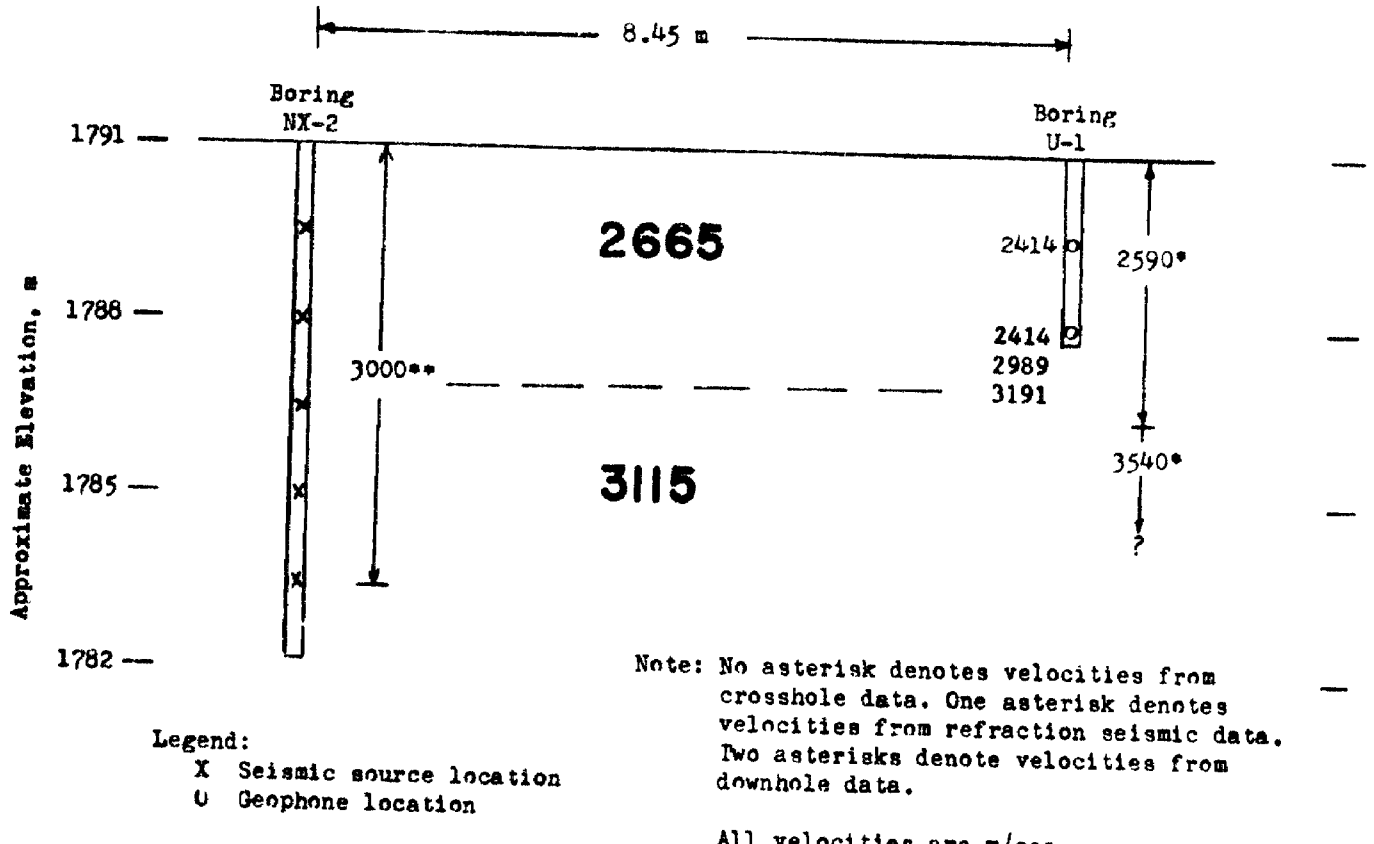

Figure 2.12. P-wave velocity profile interpreted from crosshole, downhole, and surface refraction seismic test data NX-2 to U-1.

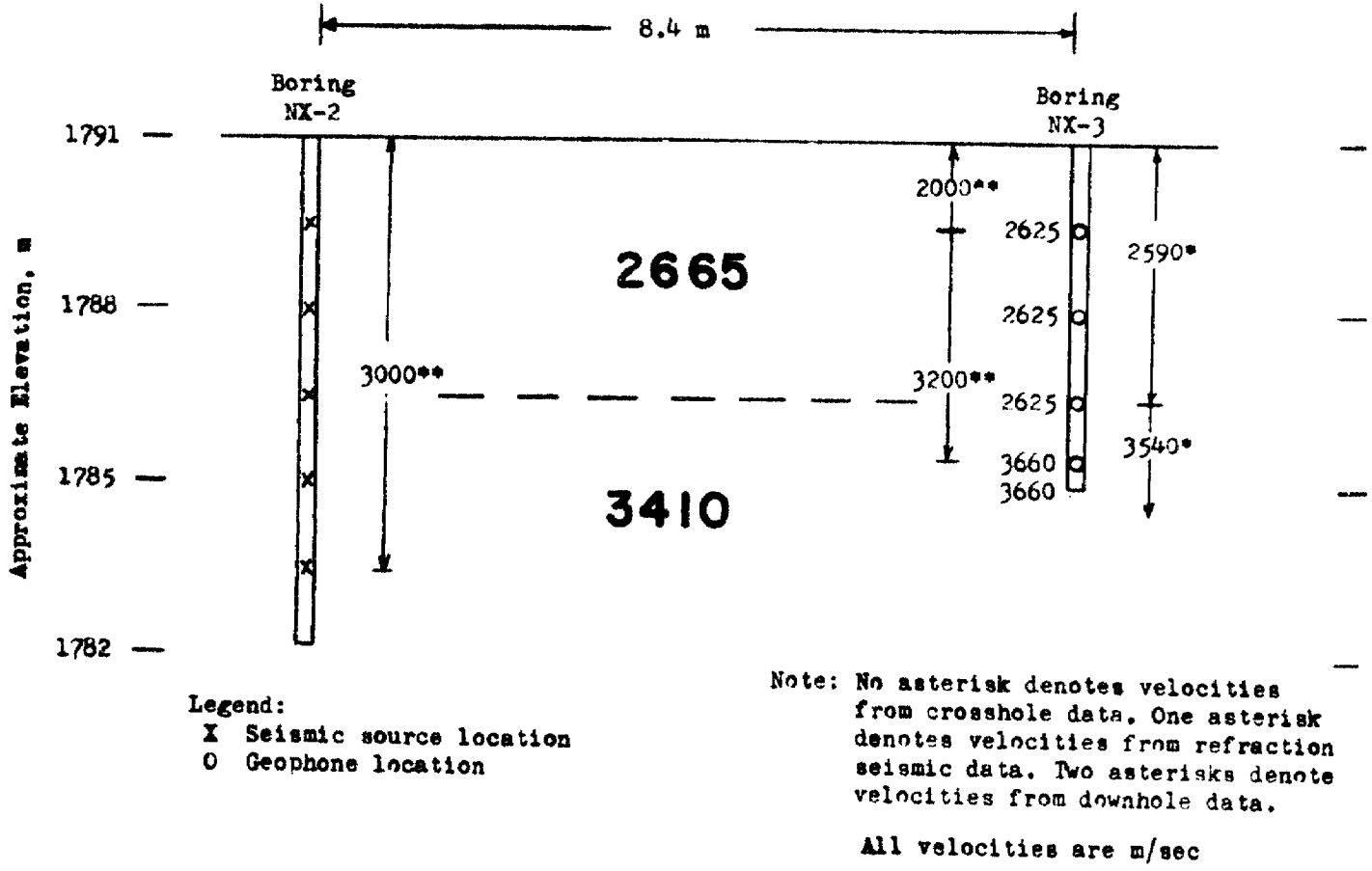

Figure 2.13. P-wave velocity profile interpreted from crosshole, downhole, and surface refraction seismic test data NX-2 to NX-3.

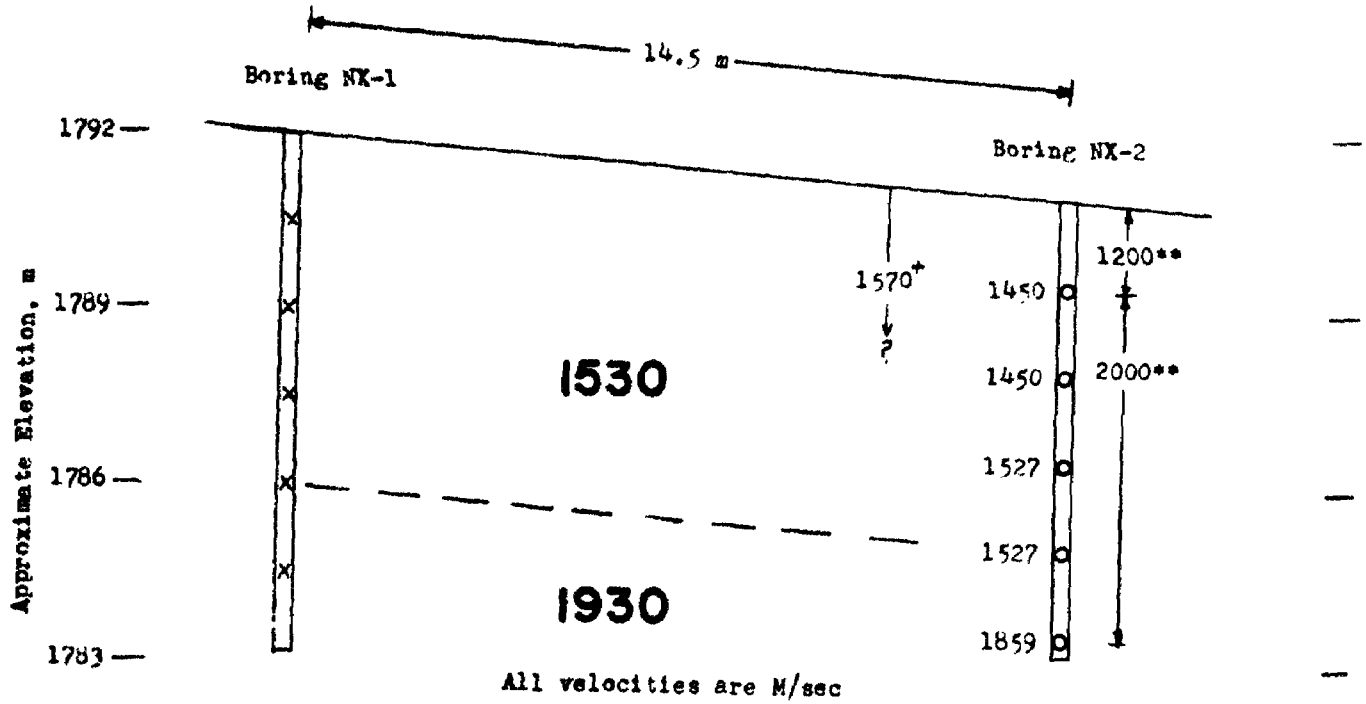

Figure 2.14. S-wave velocity profile interpreted from crosshole, downhole, and surface S-wave test data NX-1 to NX-2.

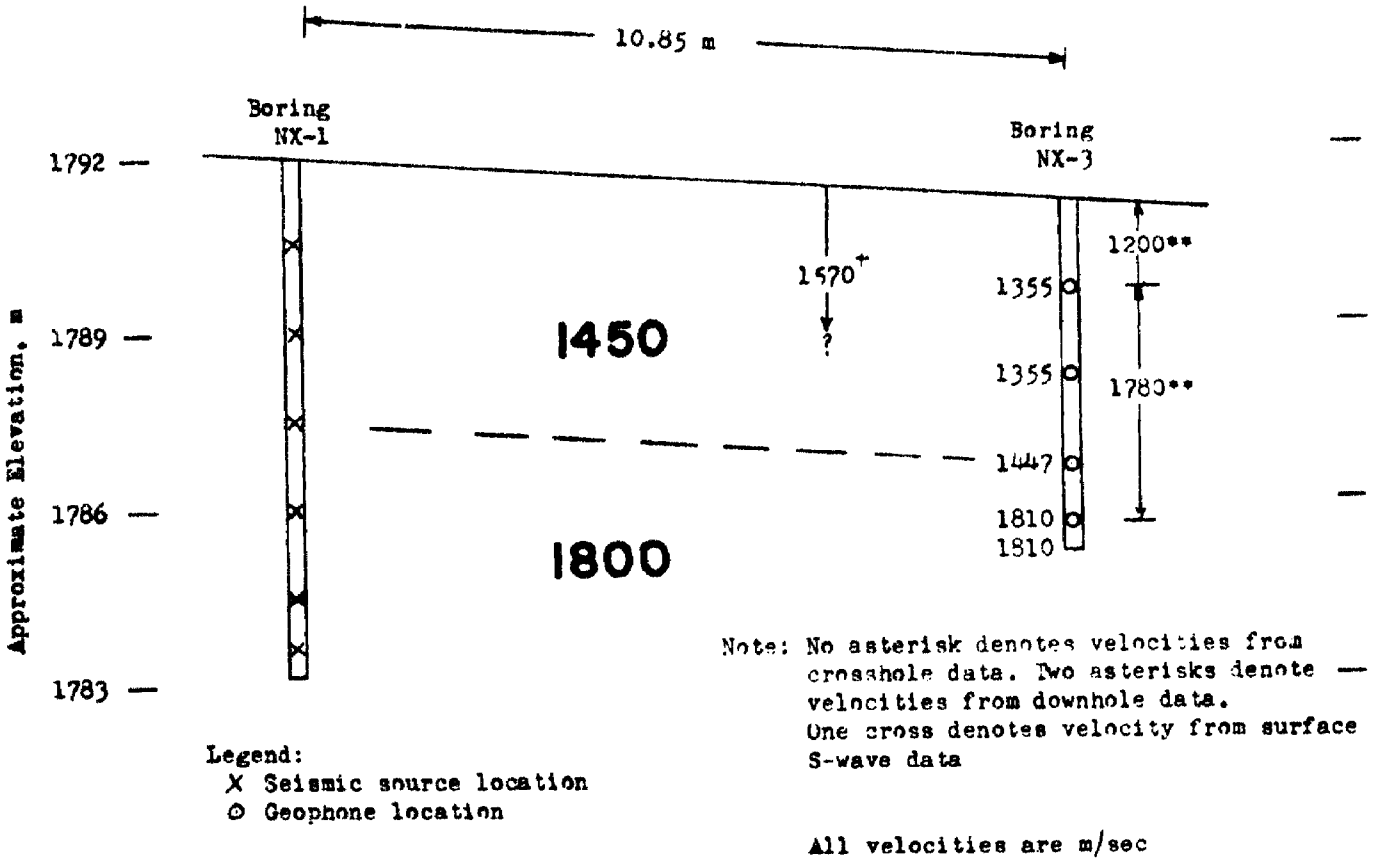

Figure 2.15. S-wave velocity profile interpreted from crosshole, downhole, and surface S-wave test data NX-1 to NX-3.

CHAPTER 3

LABORATORY TEST PROGRAM AND RESULTS

3.1 CLASSIFICATION AND COMPOSITION TESTS

Standard laboratory classification and composition tests were performed on selected specimens of the core samples (as received in the laboratory) to determine wet density, water content, dry density, and specific gravity of solids. Results of these tests are plotted in Figures 3.1 and 3.2 as a function of depth. Figure 3.3 shows the calculated volume of voids and the calculated volume of air for selected depths.

3.2 ULTRASONIC WAVE VELOCITY AND UNCONFINED COMPRESSIVE STRENGTH DETERMINATION

Selected specimens of core from the three NX boreholes were cut to 10.7-centimetre lengths and the cut ends finished with a precision surface grinder. The compression and shear wave velocities were then determined in the axial direction, and the results are plotted as a function of depth in Figure 3.4. The ultrasonic velocities exceed the P- and S-wave velocities interpreted in Figures 2.13-2.15. This trend has been noted in other comparisons of field and laboratory wave velocity data.[1,3]

After completion of the ultrasonic velocity tests, the specimens were tested in uniaxial compression to determine their unconfined compressive strengths. The results of these latter tests are also plotted in Figure 3.4, where it should be noted that for two of the specimens the strength value is in excess of 1.1 kbar while the minimum strengths exceeded 0.3 kbar. The figure shows a significant increase in strength at the 3-metre depth.

3.3 PETROGRAPHY

As indicated in Figure 2.3, the primary rock types at the site are medium-grain, red sandstone in the upper 4 metres and dense, red siltstone below 4 metres. The exceptions to this were the irregular-shaped pockets

of light tan to white sandstone and siltstone scattered throughout the core and a thin seam of weathered shale at 8 metres depth. In order to better categorize the rock at the site, a limited petrographic examination was conducted on the rock found near the surface at the site, i.e., the sandstone member.

The petrographic examination of a disaggregated sample of surface rock from the site revealed an approximate composition of 68 percent quartz, 29 percent undifferentiated feldspar, and 3 percent unknowns. There were no detectable rock fragments in the sample. The quartz grains were generally coated with iron oxide. K-feldspar was the most common feldspar, with most of the grains being weathered. Cements present in nondisaggregated samples were calcite, particularly in light colored areas, and iron oxide. Some cementitious effects, however, may be imparted by the silty-clay matrix (fines). An examination of the grain-size distribution reveals a mean grain size of 0.13 millimetre with a standard deviation of 0.59 millimetre (moderately sorted) and 16 percent fines. Individual grains do not possess particularly high sphericity (subrounded to subangular). The compositional and textural classification of the rock would be an immature, red, fine-grained arkose.

3.4 OTHER MECHANICAL PROPERTY TESTS

3.4.1 Test Program. In addition to the ultrasonic wave velocity measurements and unconfined compression tests discussed in Section 3.2, a few other mechanical property tests were conducted on specimens from the upper 3 metres of borings NX-1 and NX-3. The program consisted of static and dynamic* isotropic (hydrostatic) compression (IC) tests and

* For purposes of this study, static tests are defined as those with strain rates of 10^{-4}/sec or a stress rate of approximately 1 kbar/min. Dynamic tests are defined as tests in which the stress rate is approximately 0.3 kbar/msec and in which inertial stresses are negligible.

triaxial compression (TX) tests. Table 3.1 outlines the test program. Specimen preparation and handling techniques and details of the WES dynamic high-pressure triaxial test device (which was used for all of the IC and TX tests) can be found in previous WES publications.[3,5,6]

3.4.2 Isotropic Compression Test Results. Data plates for one static and two dynamic isotropic compression tests are presented in Figures 3.5-3.7. Another source of isotropic compression data is from the confining pressure application phase (hydro-phase) of TX tests; these data are plotted in Figure 3.8 together with static and dynamic IC test results. The curves appear to group according to borehole, with specimens from NX-1 being more compressible than those from NX-3. The IC test results presented in Figures 3.5 and 3.6 were obtained on the same specimen: static IC followed by dynamic IC. These results are replotted in Figure 3.9 as if part of a single, cycled IC test. The curves are essentially parallel above 0.1 kbar indicating that rate effects on the bulk modulus are negligible in the range investigated.

3.4.3 Triaxial Compression Test Results. Data plates for static triaxial compression tests are presented in Figures 3.10-3.13. Figures 3.14-3.17 are data plates for the dynamic triaxial compression tests.* Note in Figure 3.17 that test DTX/NX3/5.6(B) was conducted, at a lower confining pressure, on the same specimen as test DTX/NX3/5.6(A) (Figure 3.16).

3.4.4 Hollow Cylinder Test Results. Four tests were conducted on 6.2-centimetre-long NX specimens with 0.62-centimetre-diameter holes along the axis. The internal pressure required to rupture the hollow cylinder is determined and the results used to compute the tensile strength. The average tensile strength determined from the four tests is $\sigma_T = -0.038$ kbar.

---

* σ_1 and ε_1 are stress and strain in the axial direction. σ_3 and ε_3 are stress and strain in the radial direction. $\sqrt{3J_2'} = \sigma_1 - \sigma_3$ for the TX test, where J_2' is the second invariant of the deviatoric stress tensor.

3.5 FAILURE DATA

The maximum principal stress difference ($\sigma_1 - \sigma_3$) and corresponding mean normal stress ($\frac{\sigma_1 + 2\sigma_3}{3}$) data from each TX test and the tensile strength can be used to define a failure envelope for the material. Figure 3.18 presents the failure data points and a "best fit" curve to all the points (solid line). A "best fit" curve to the three dynamic failure points (dashed curve) lies slightly above the other curve.

TABLE 3.1 OTHER TESTS CONDUCTED

Test Type	Static (S) or Dynamic (D)	No. of Tests	Specimen Size	Remarks
IC	S, D	2	NX by 7.62 cm	Static isotropic (hydrostatic) compression load-unload cycle to 0.55 kbar followed by a dynamic isotropic compression cycle to 0.62 kbar on the same specimen. LVDT's used to measure deformations.
IC	D	1	NX by 7.62 cm	Dynamic isotropic compression test to 0.62 kbar.
TX	S	4	NX by 12.7 cm	Triaxial compression tests. Confining pressures of 0.035, 0.07, and two tests at 0.14 kbar. Confining pressure and axial load cycled at about one-half the peak values. LVDT's used to measure deformations. Undrained tests.
TX	D	4	NX by 12.7 cm	Triaxial compression tests. Confining pressures of 0, 0.03, 0.08, and 0.14 kbar. The tests at confining pressures of 0.08 and 0.14 kbar were conducted on the same specimen, since the specimen did not fail at 0.14-kbar confining pressure. Undrained tests.
HC	S	4	NX OD by 0.64 cm ID by 6.2 cm	Static hollow cylinder tests conducted to give an idea of the magnitude of the tensile strength. No deformation.

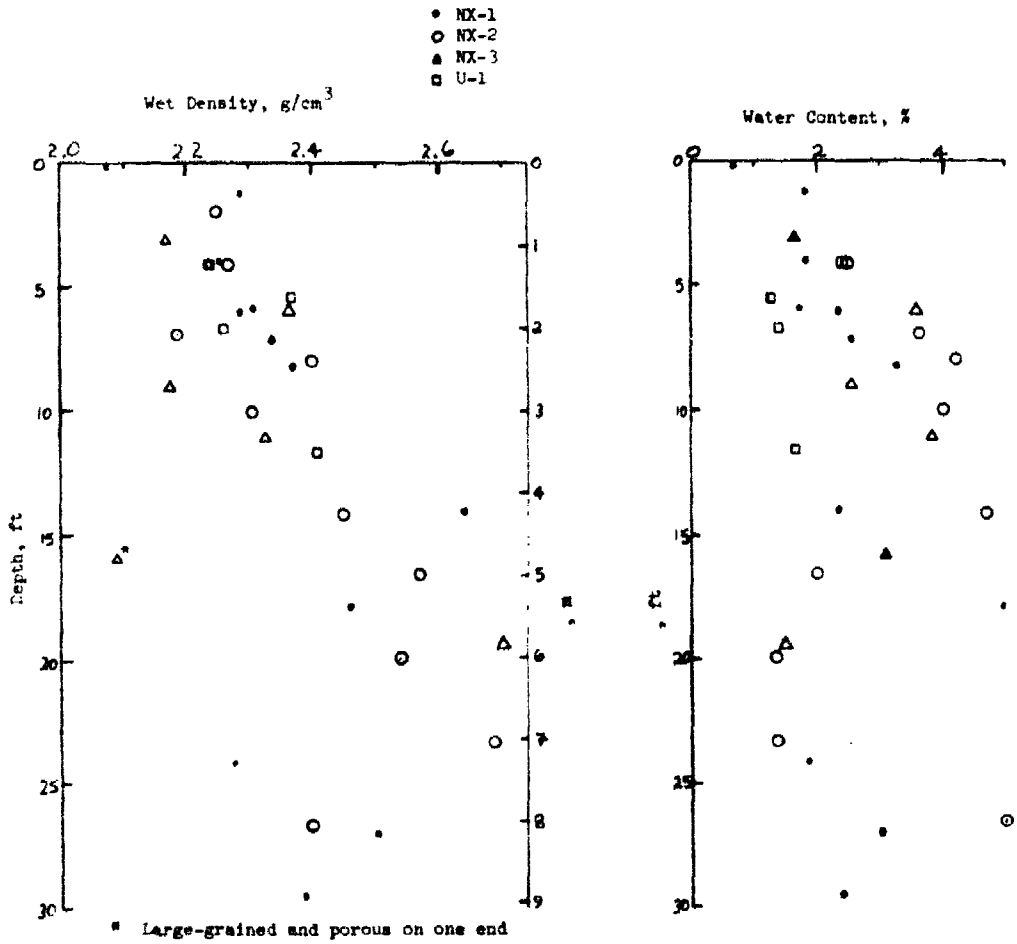

Figure 3.1. Classification and composition tests: wet density, water content.

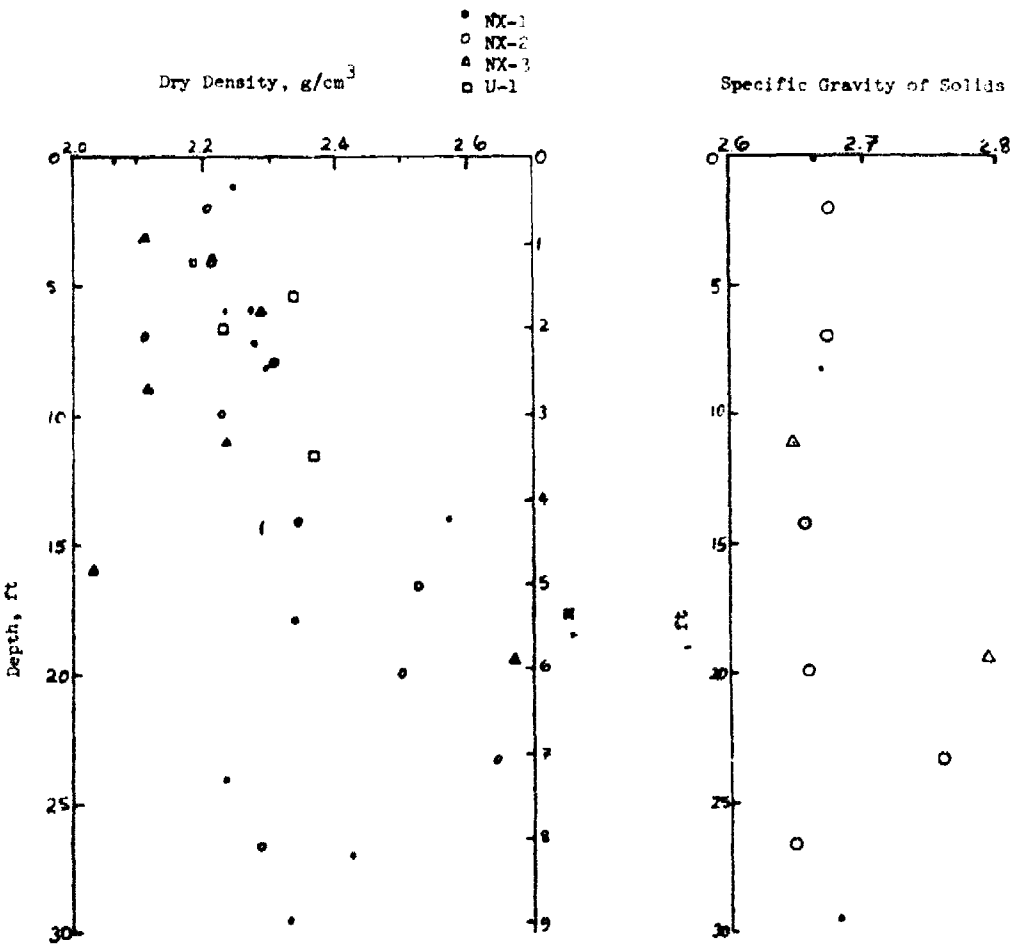

Figure 3.2. Classification and composition tests: dry density, specific gravity of solids.

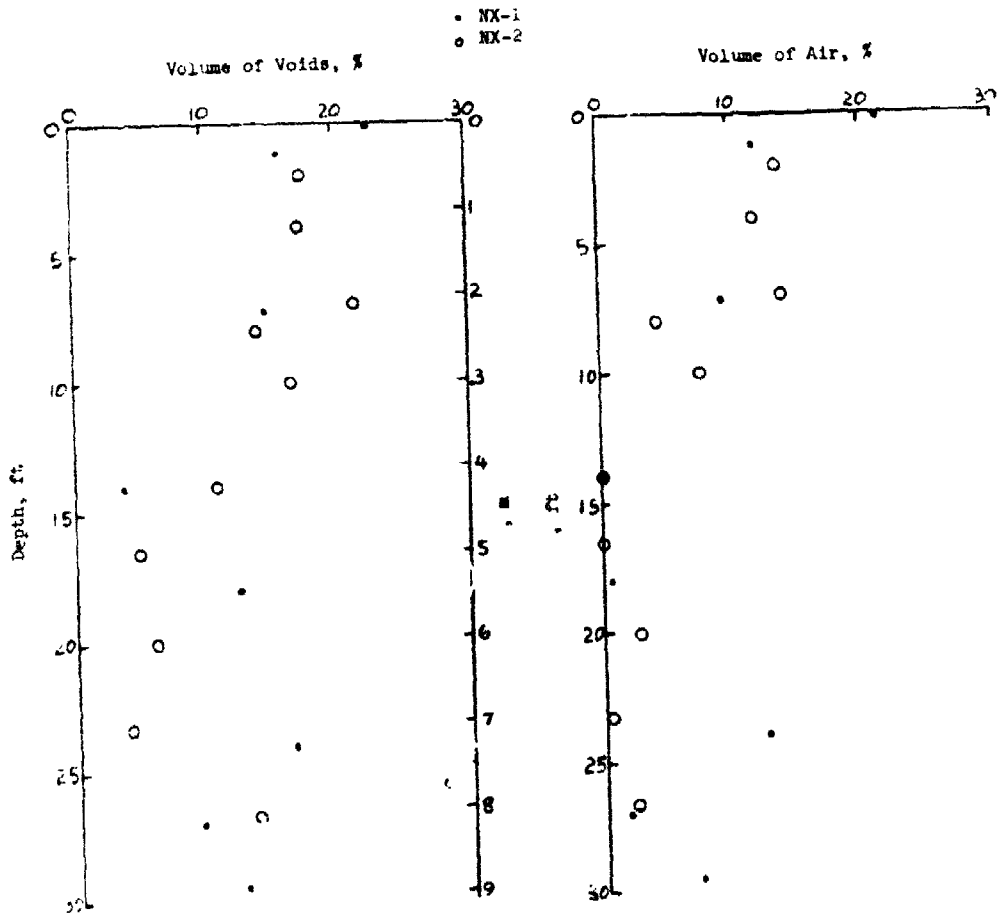

Figure 3.3. Calculated volume of voids and volume of air.

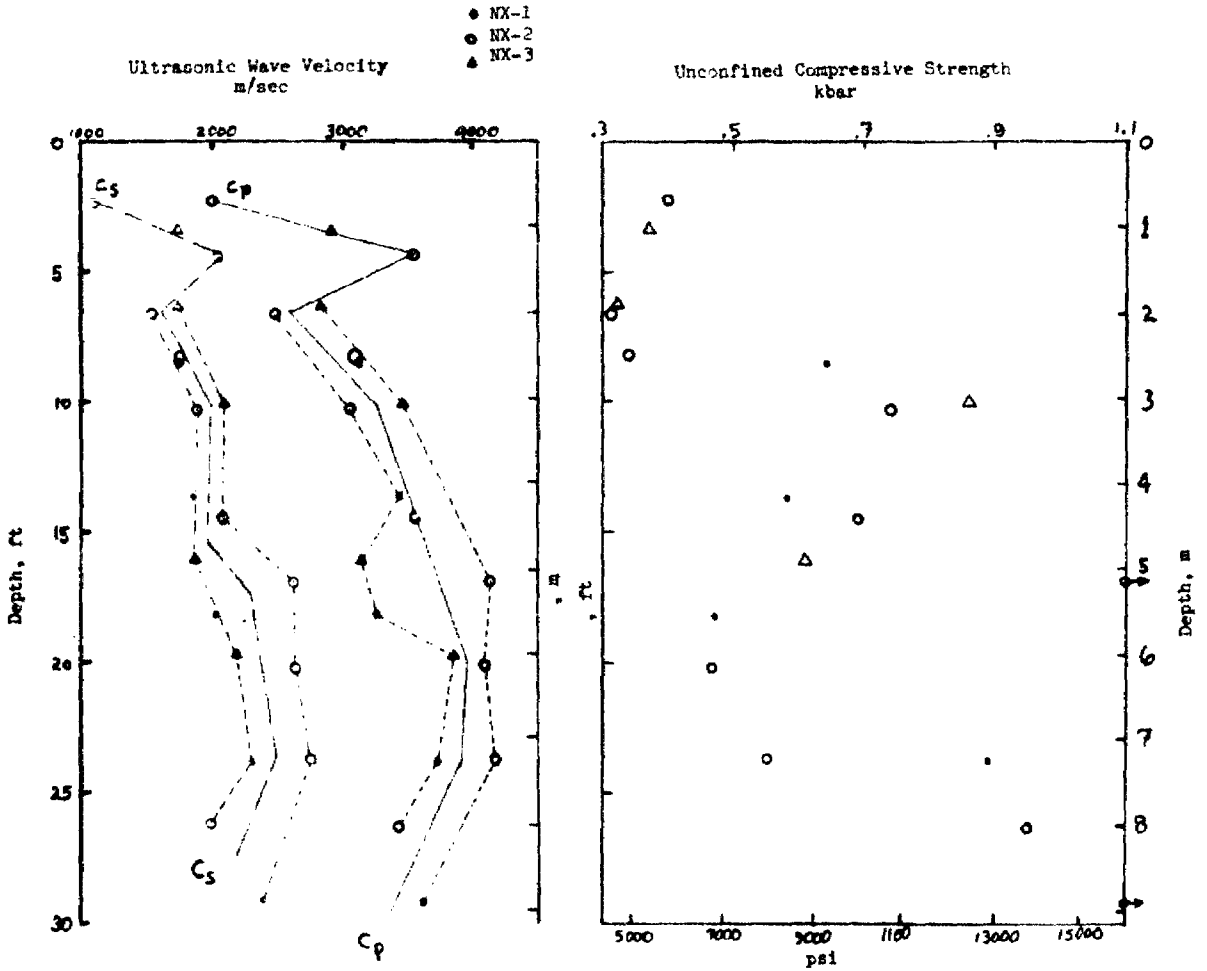

Figure 3.4. Ultrasonic wave velocities and unconfined compressive strength versus depth.

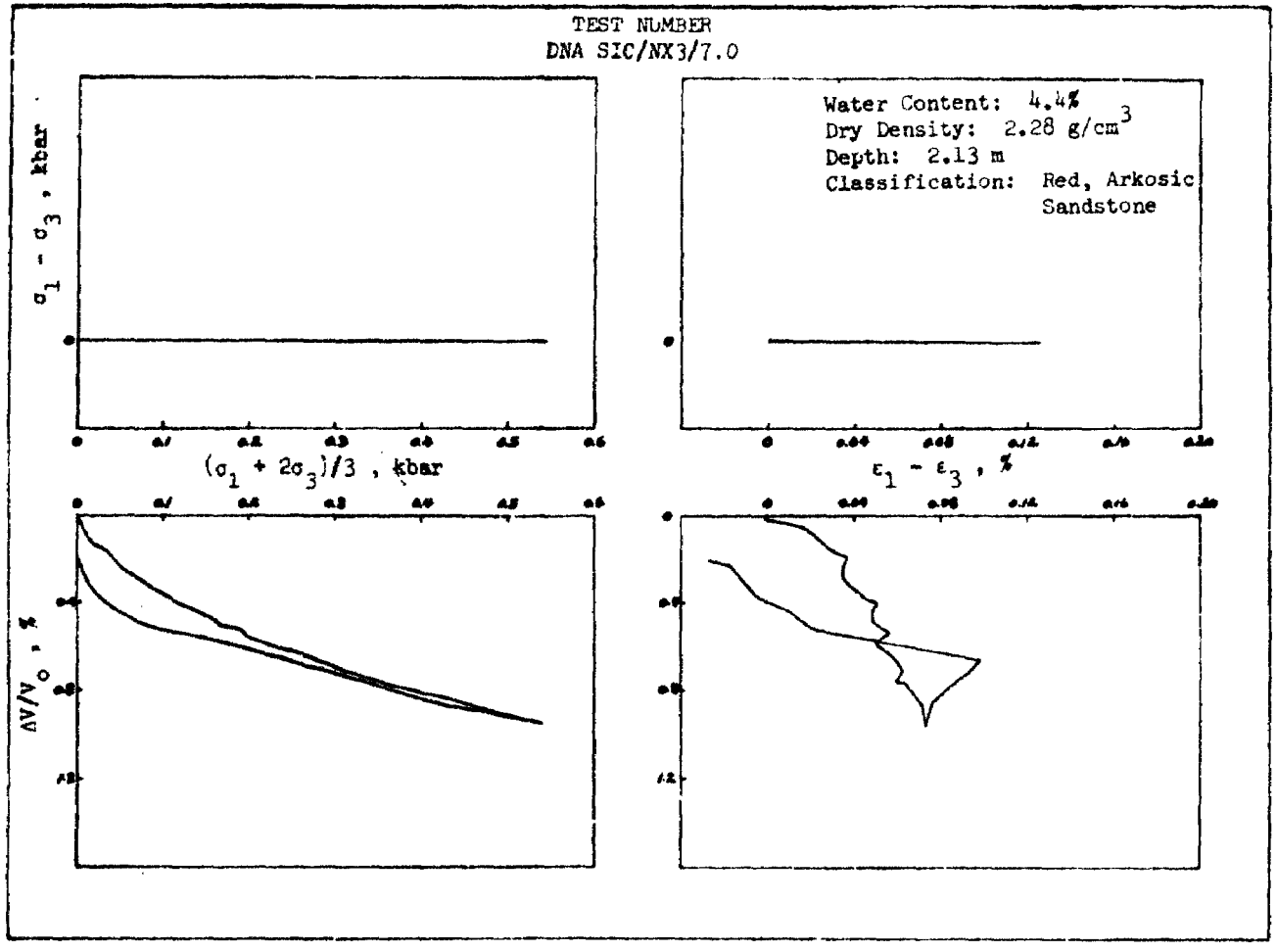

Figure 3.5. Static isotropic compression test results. Specimen NX3/7.0.

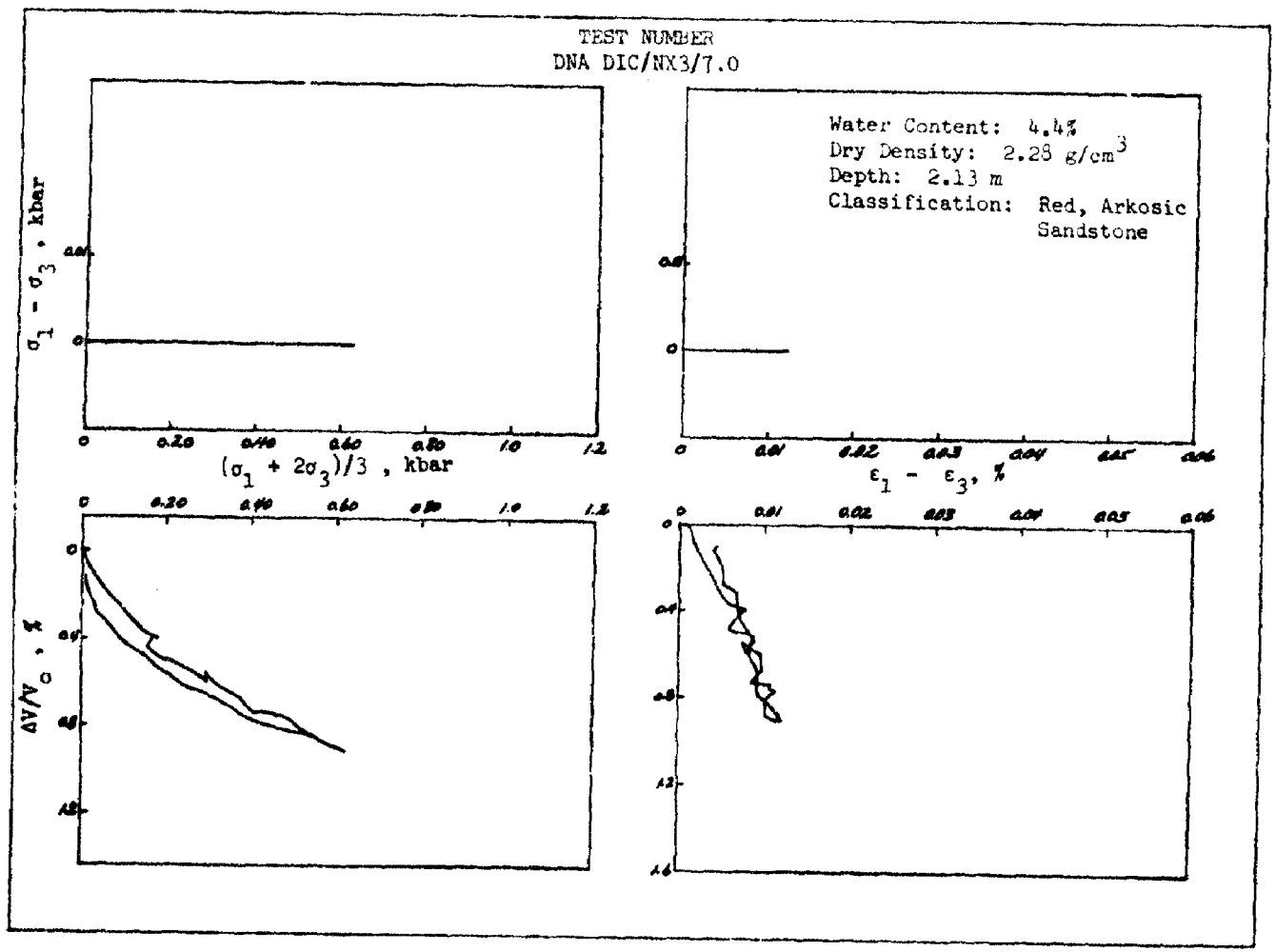

Figure 3.6. Dynamic isotropic compression test. Specimen NX3/7.0.

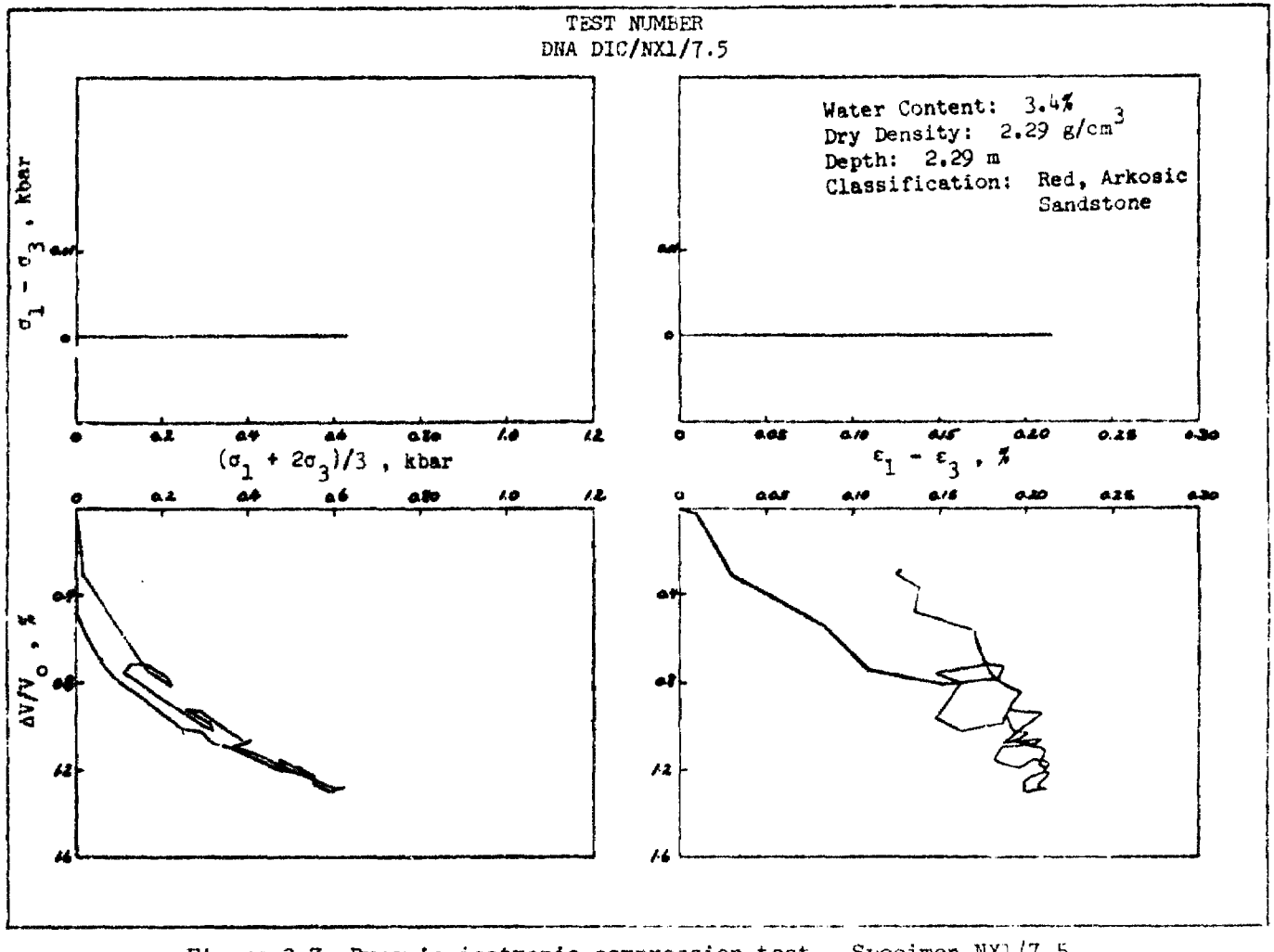

Figure 3.7. Dynamic isotropic compression test. Specimen NX1/7.5.

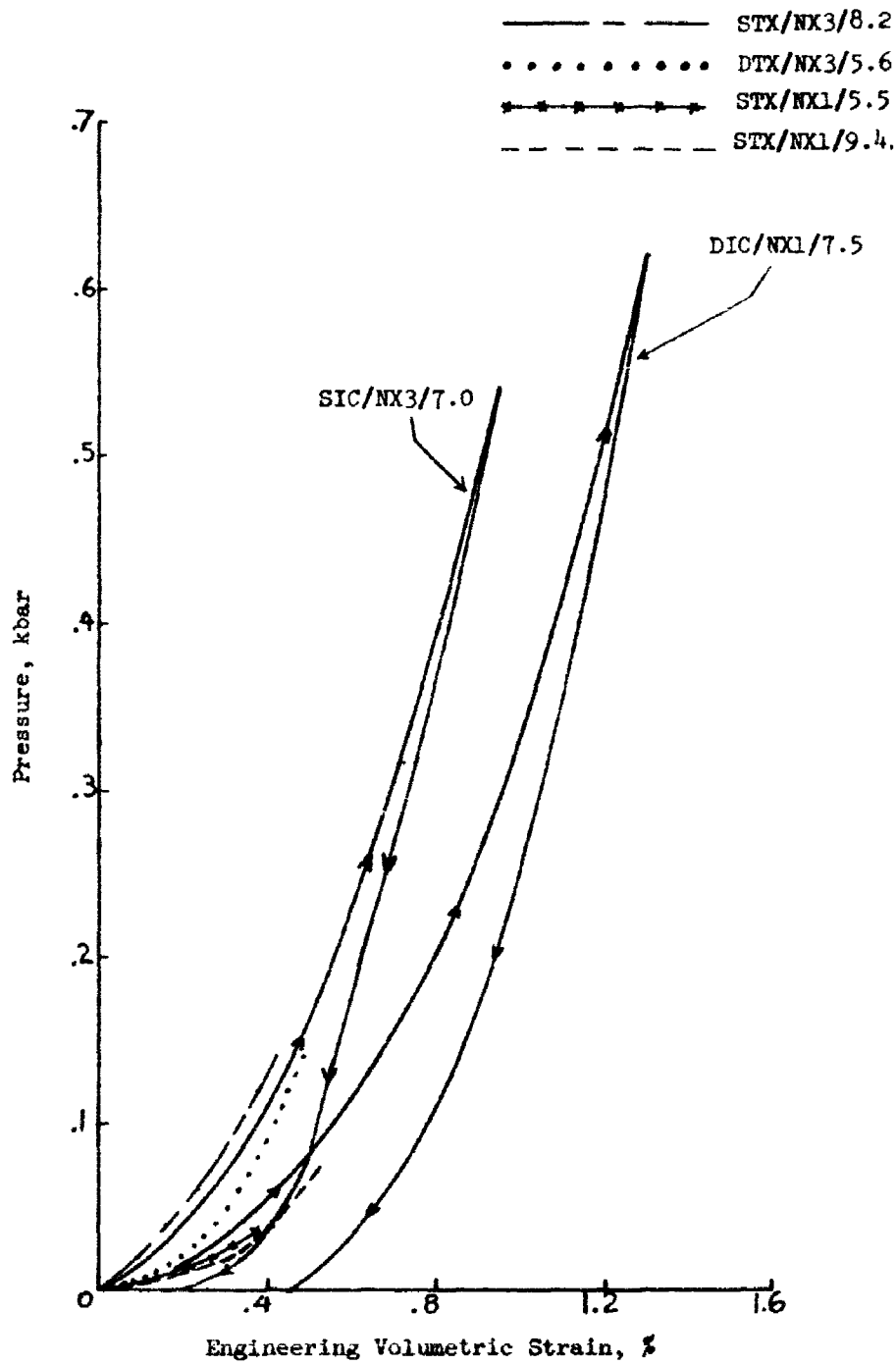

Figure 3.8. Pressure-volumetric strain response. IC tests and hydro-phase of TX tests.

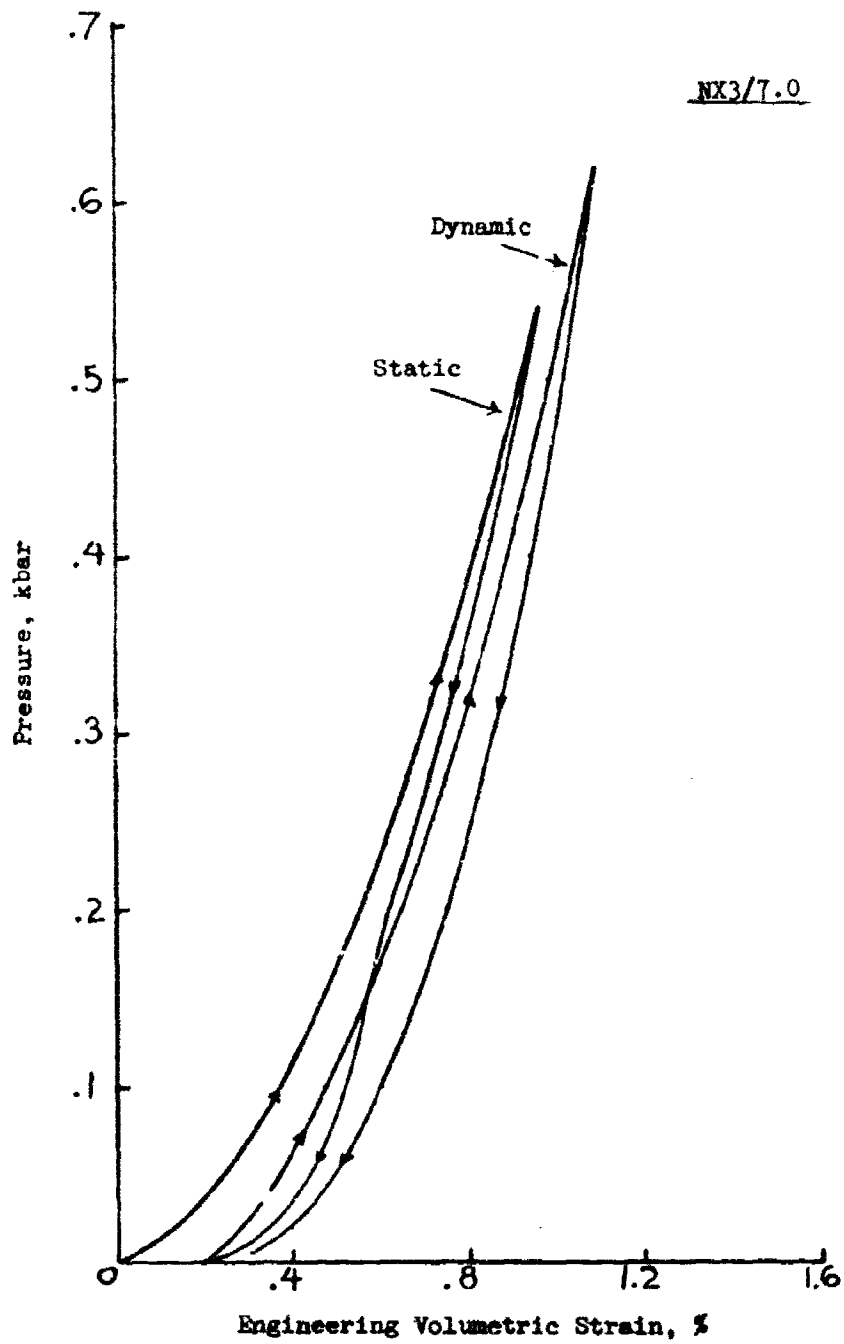

Figure 3.9. Comparison of static and dynamic response of a single rock specimen.

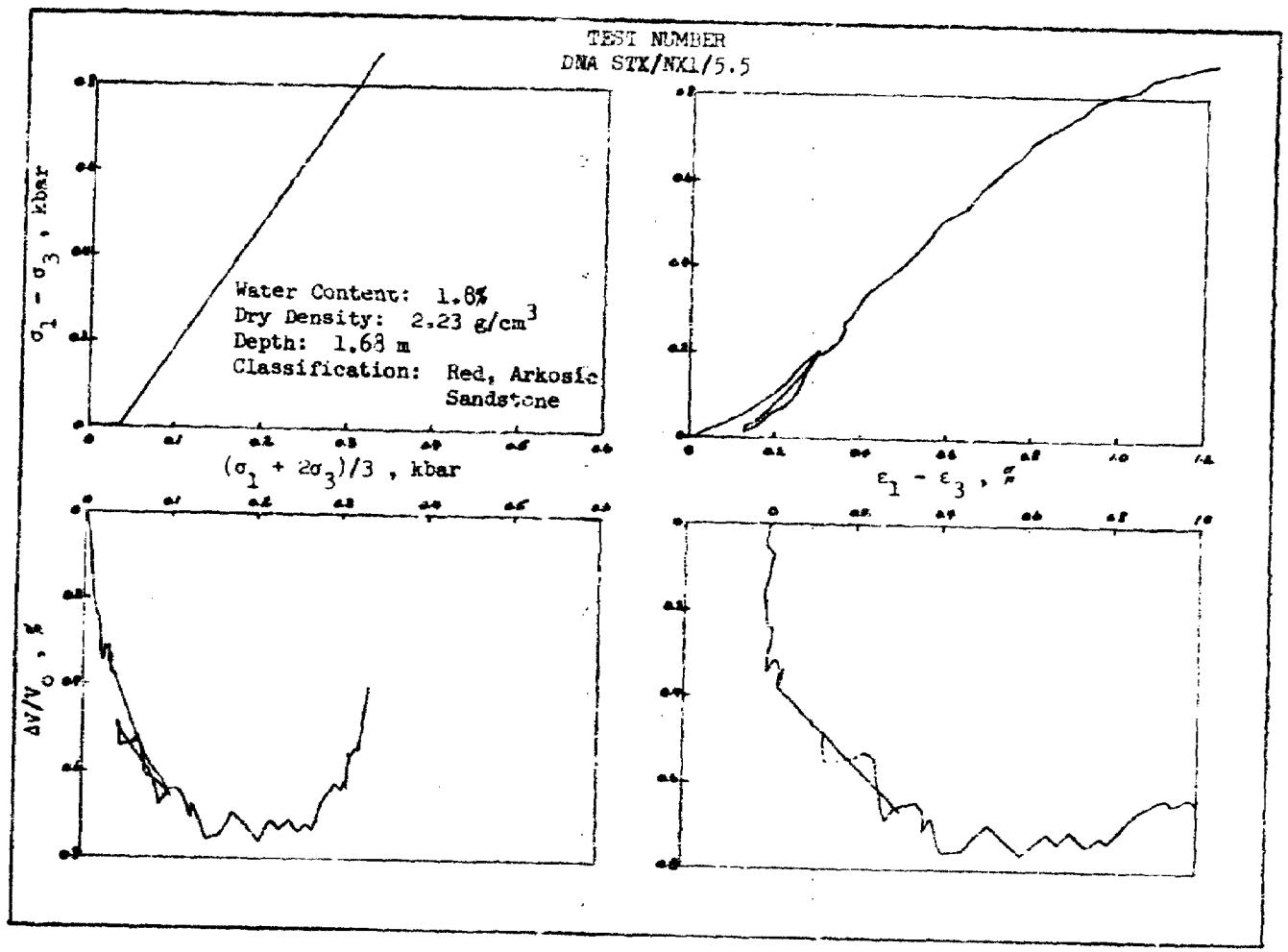

Figure 3.10. Static triaxial compression test. Specimen NX1/5.5.

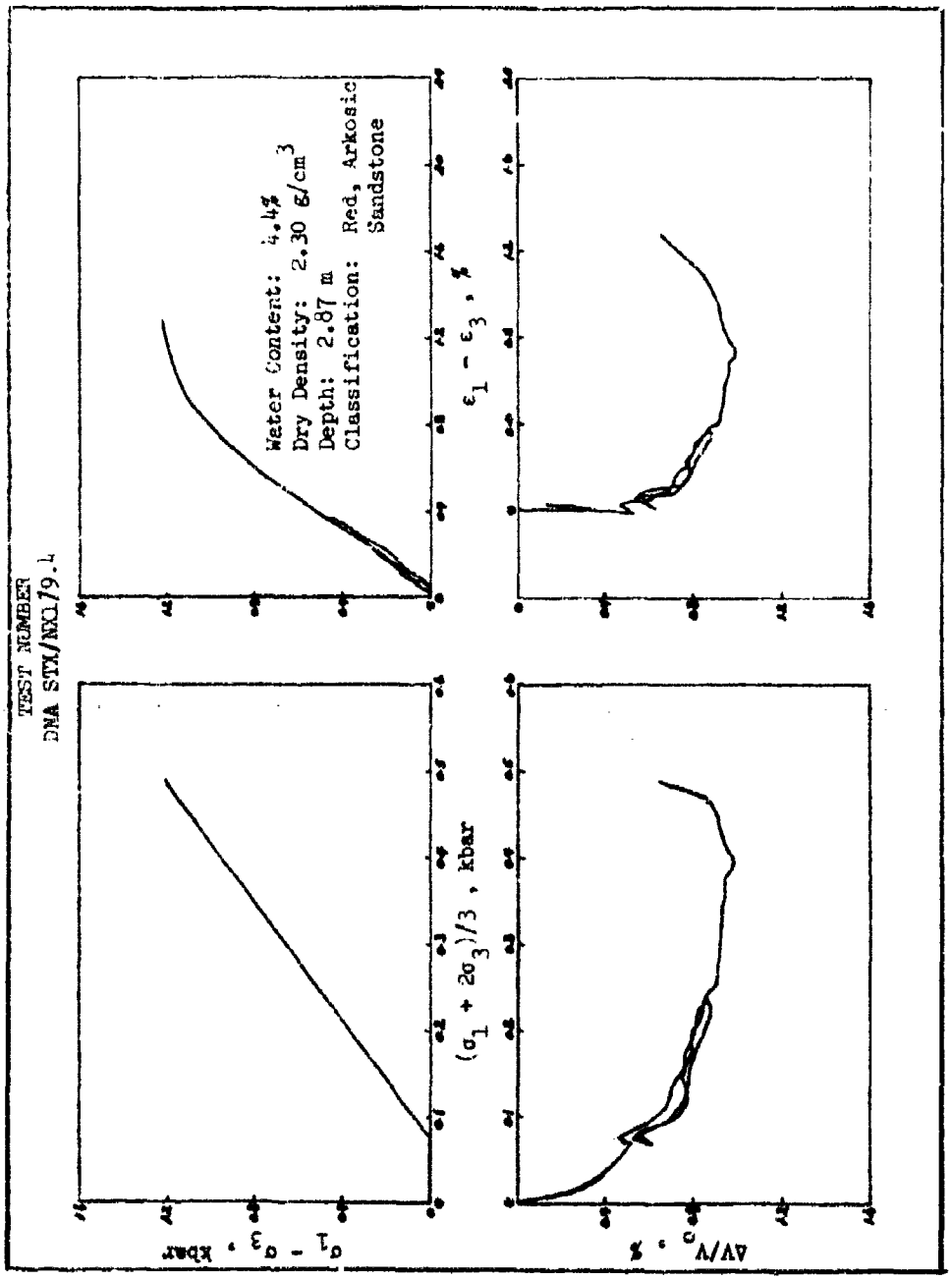

Figure 3.11. Static triaxial compression test. Specimen NX1/9.4.

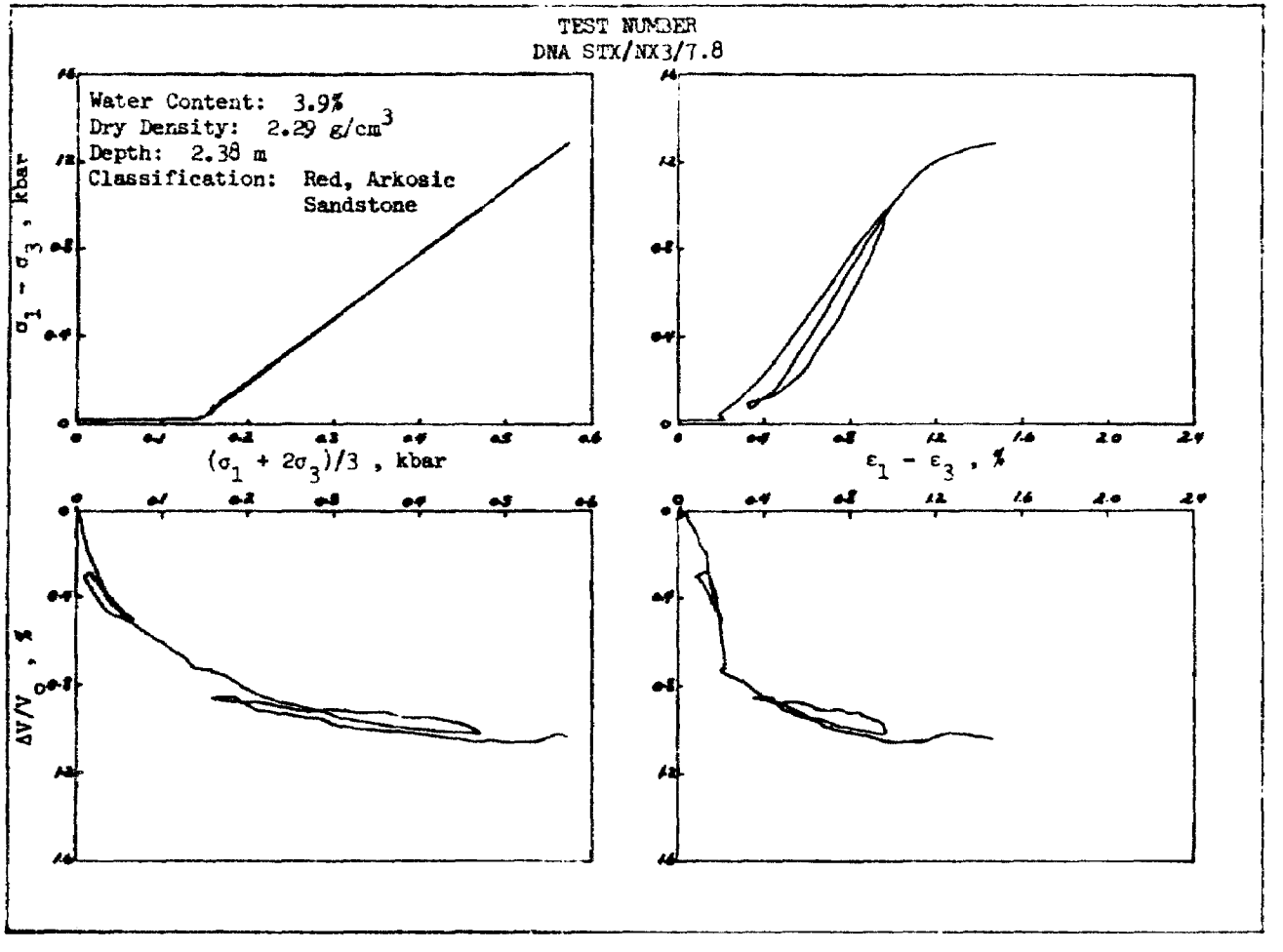

Figure 3.12. Static triaxial compression test. Specimen NX3/7.8.

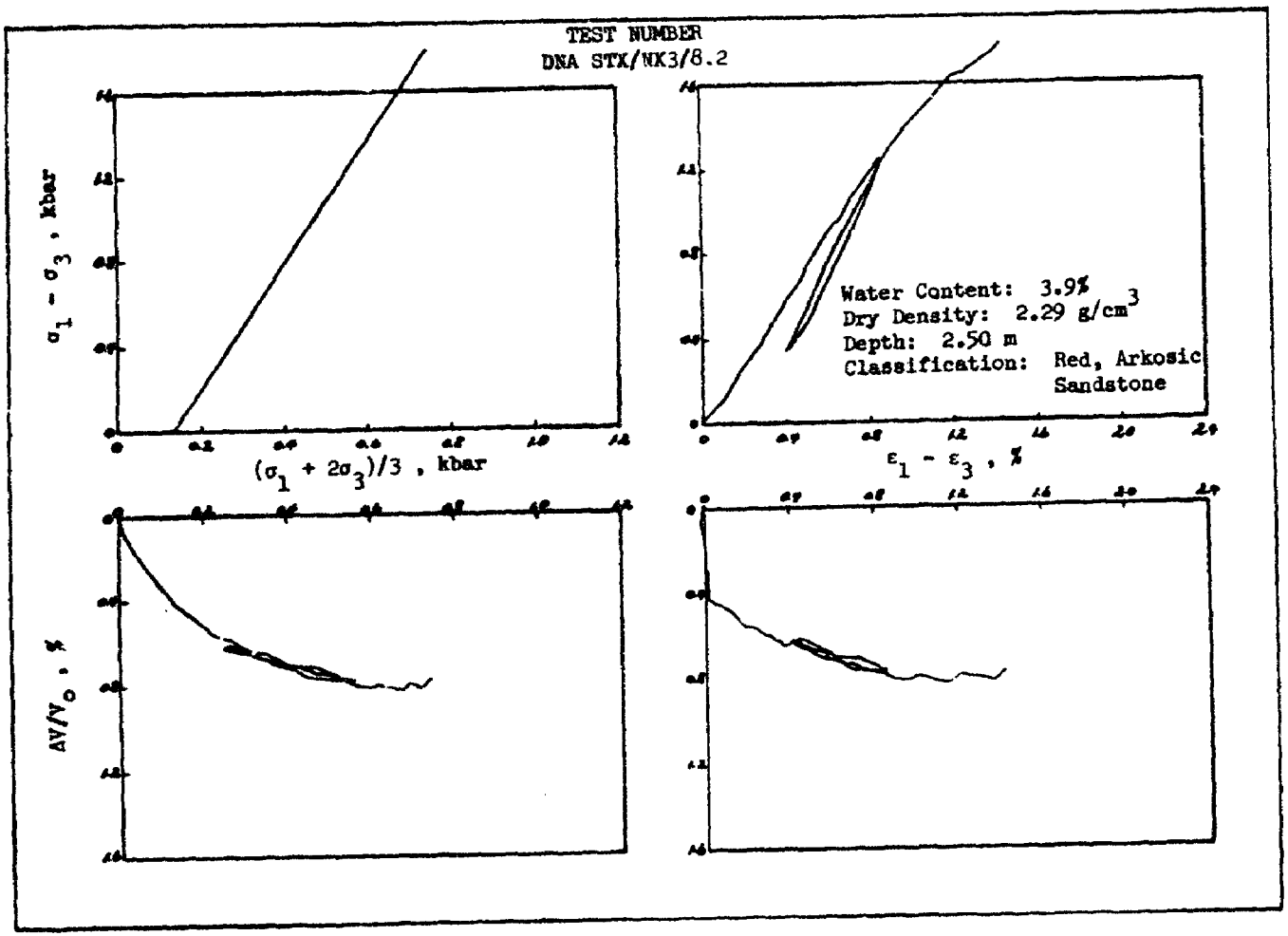

Figure 3.13. Static triaxial compression test. Specimen NX3/8.2.

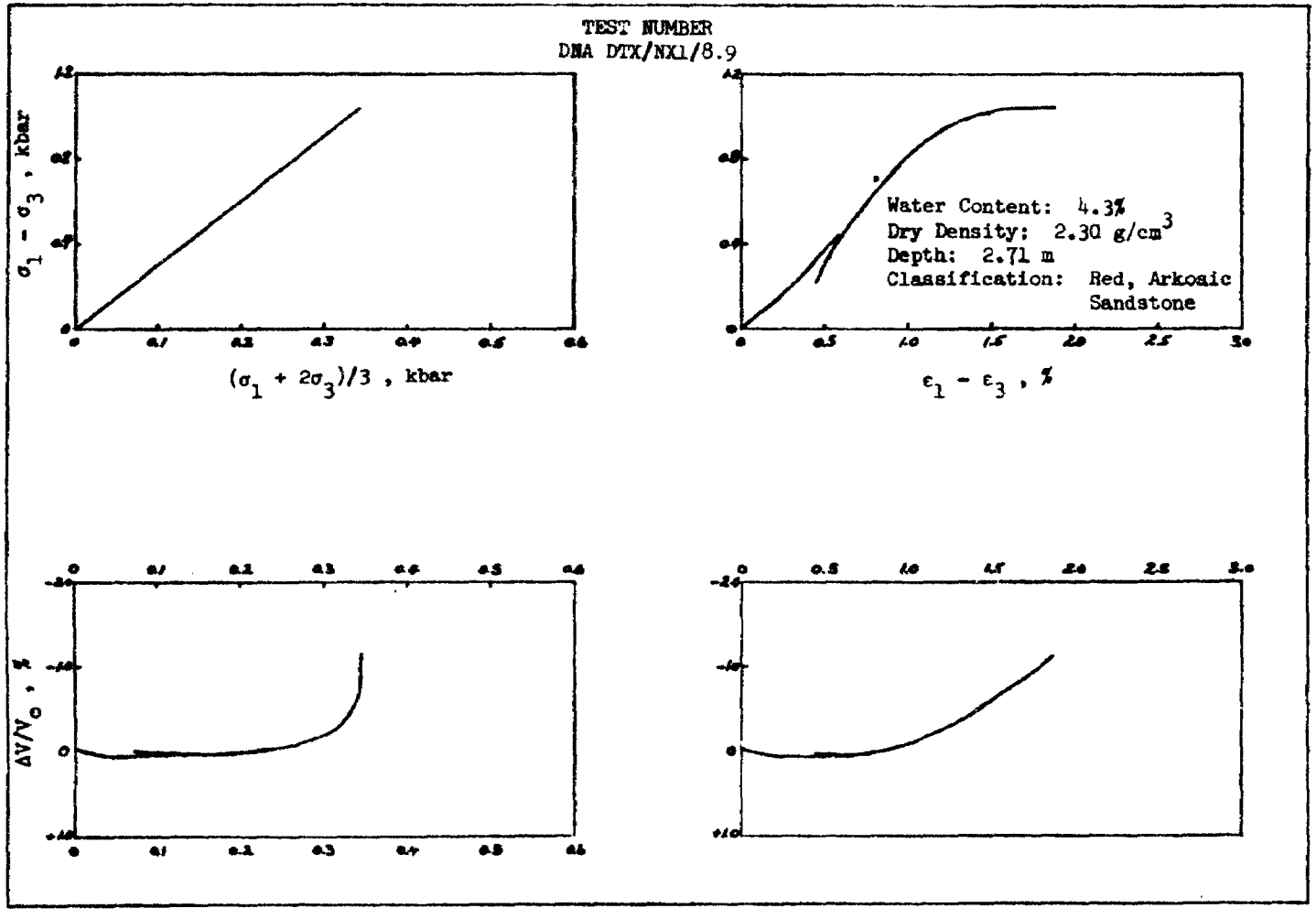

Figure 3.14. Dynamic triaxial compression test. Specimen NX1/8.9.

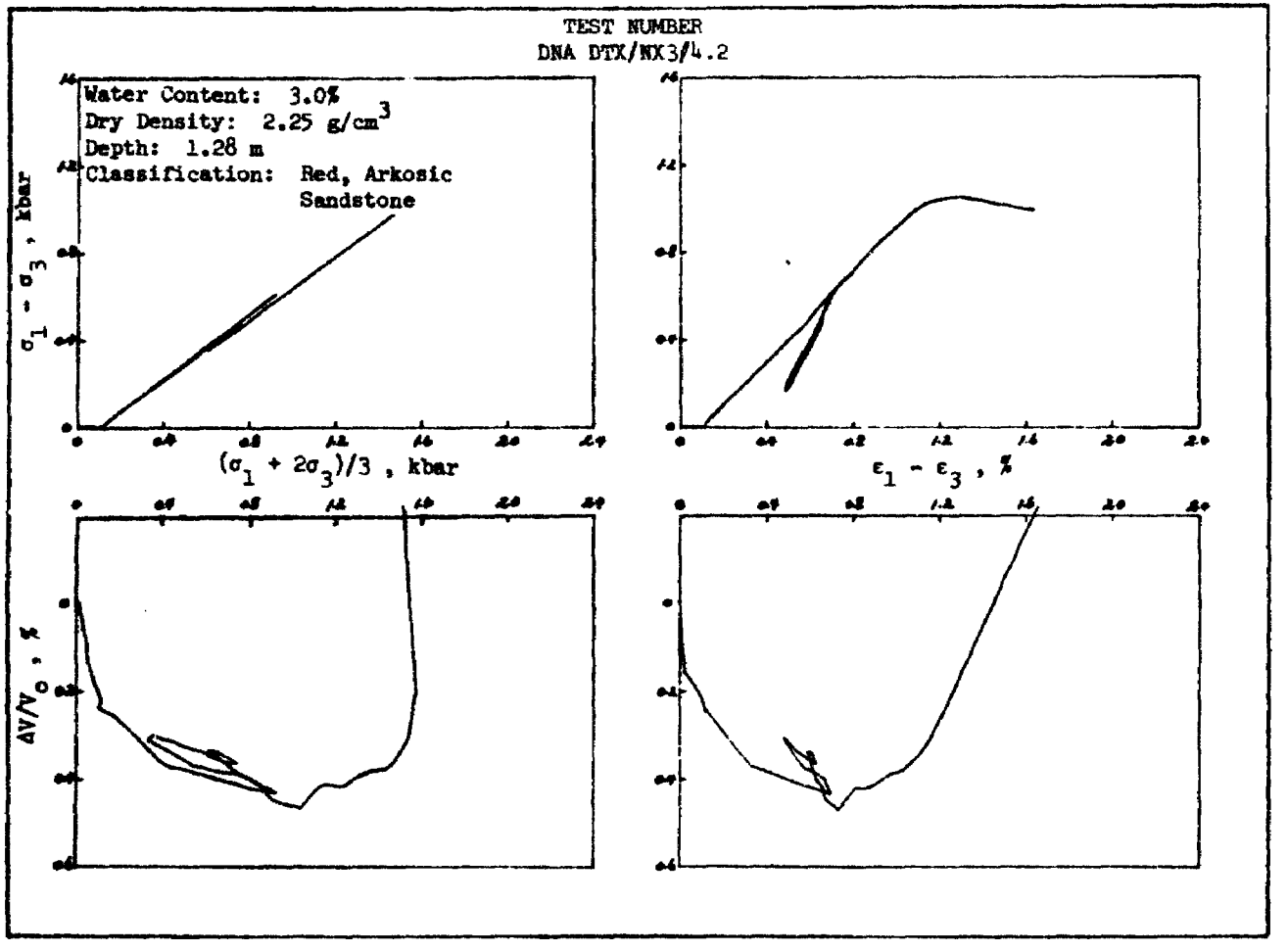

Figure 3.15. Dynamic triaxial compression test. Specimen NX3/4.2.

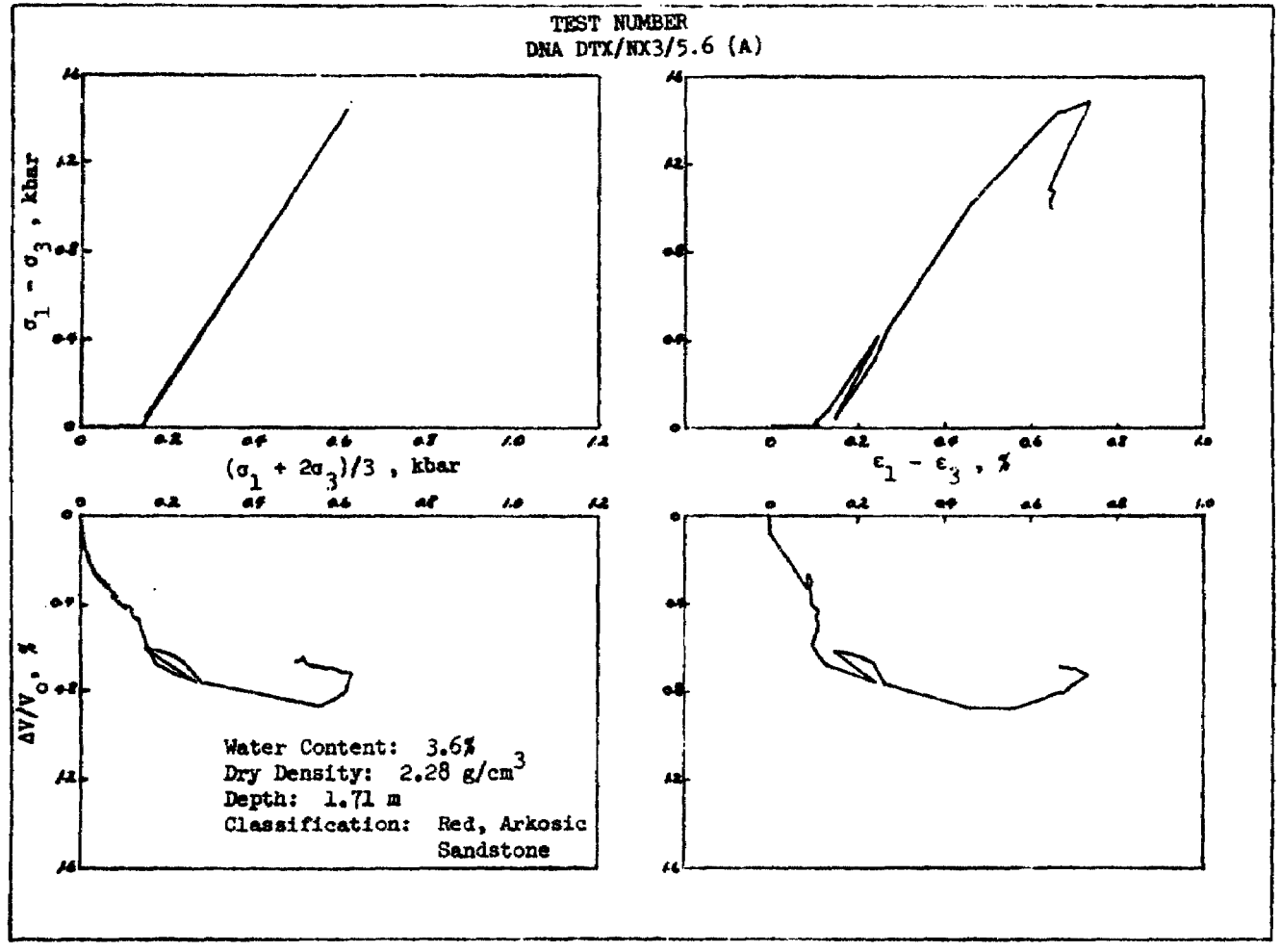

Figure 3.16. Dynamic triaxial compression test. Specimen NX3/5.6.

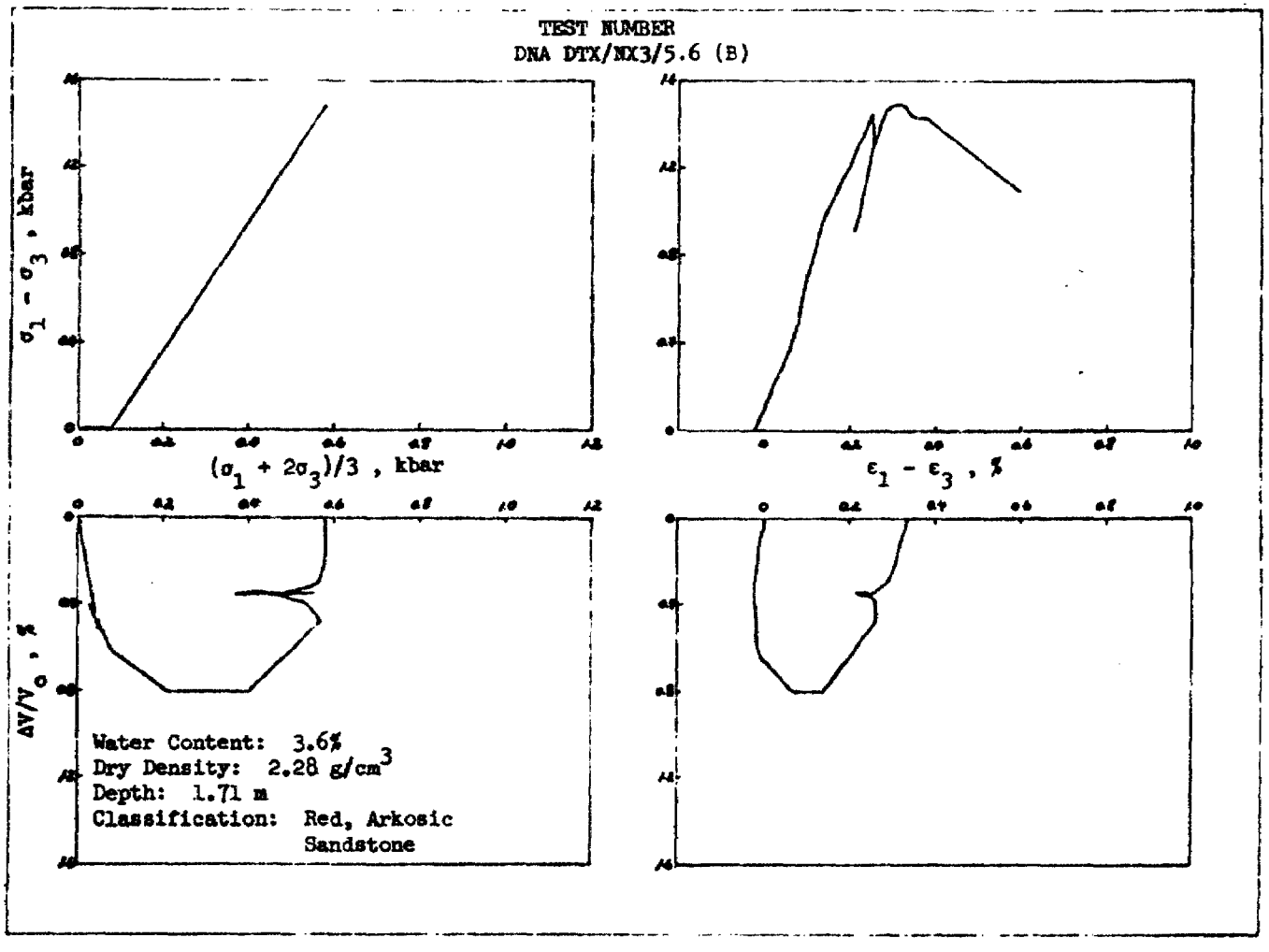

Figure 3.17. Dynamic triaxial compression test. Specimen NX3/5.6.

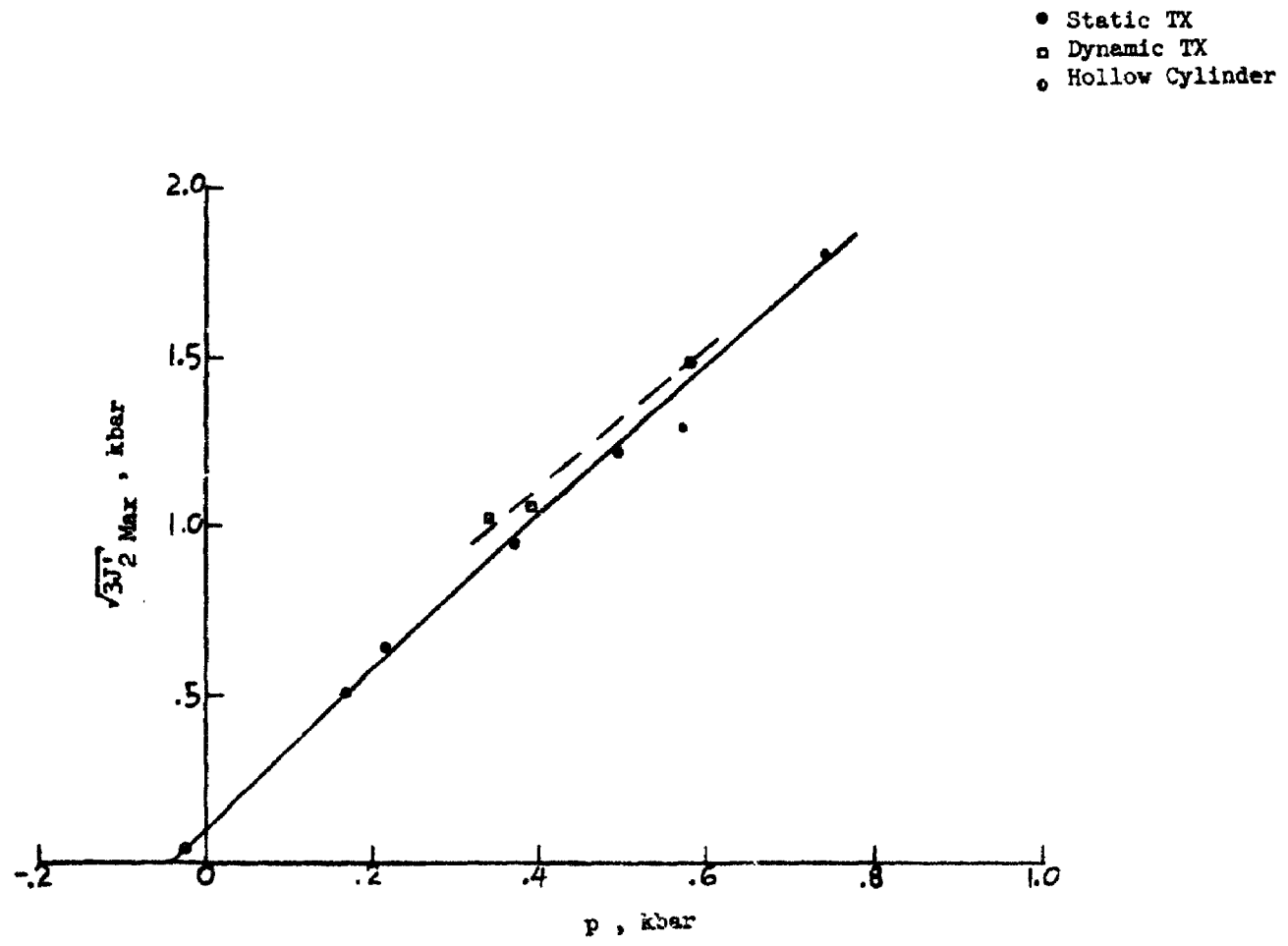

Figure 3.18. Failure data for specimens from the upper three metres of the Los Lunas site.

CHAPTER 4

SUMMARY

Results of a field investigation at a proposed DNA full-scale rock penetration site near Los Lunas, New Mexico, and of classification, composition, and mechanical property tests on rock from the site are presented. Mechanical property tests were conducted on material from the upper 3 metres of the site, where the rock is a fine- to medium-grain, red, arkosic sandstone member of the Yeso Formation.

As a result of the strength data from the laboratory test program, it became apparent that the overall program objectives of extending the target strength range to a very-low-strength target (< 0.1 kbar) would not be achieved with the Los Lunas site. Figure 4.1 compares the unconfined compressive strength versus depth profile of the Los Lunas site with those of the San Ysidro and TTR sites. Since (1) the near-surface strength is intermediate between the strengths at sites already used for full-scale penetration tests, and since (2) a layer interface exists at the site within the depth regions which would be exercised in a penetration test (3 to 5 metres), this site is not acceptable for its originally intended purpose. Consequently, it was recommended to DNA and SLA that the remaining full-scale penetration test not be conducted at the Los Lunas site.[7] It was felt that more useful data would be generated by conducting additional tests at a higher impact velocity and possibly a test with higher obliquity (=20 degrees) at the San Ysidro site.

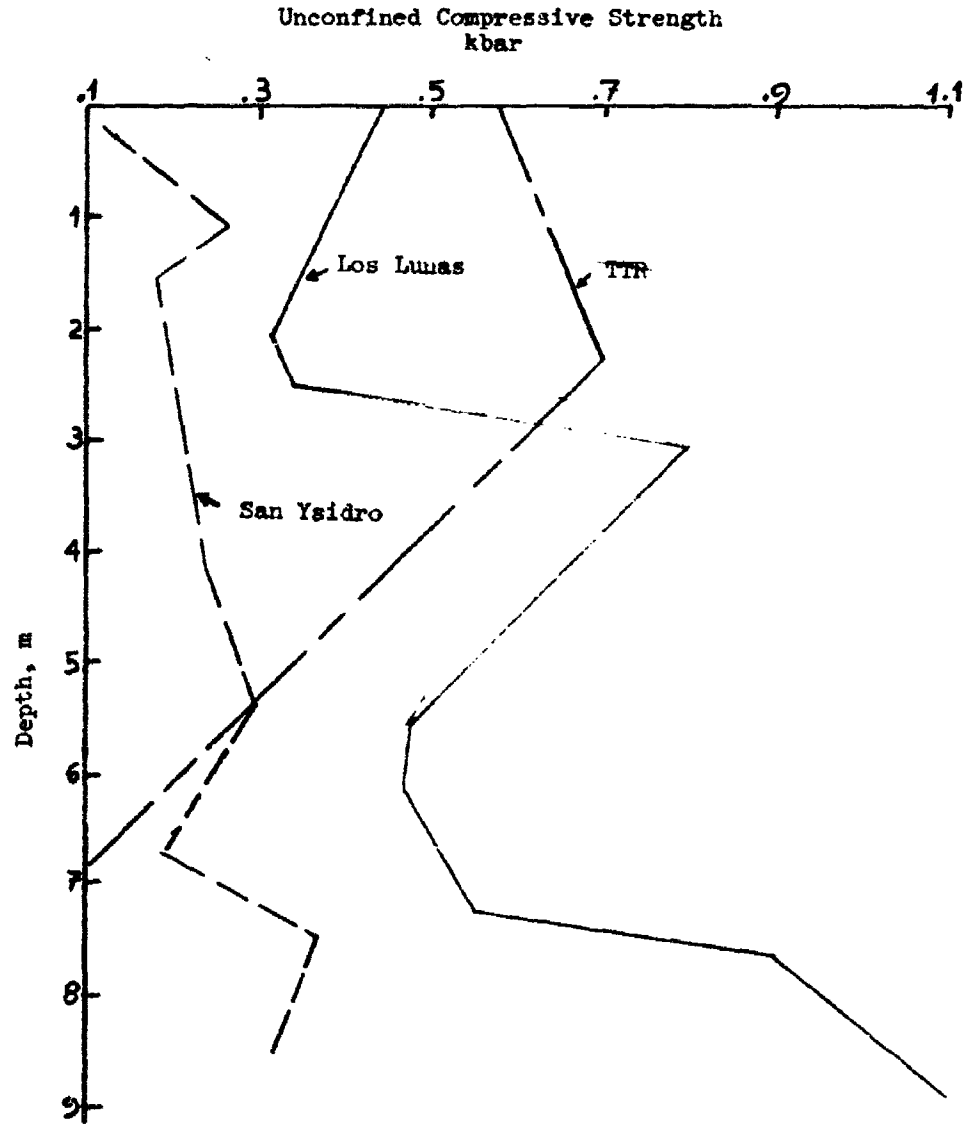

Figure 4.1. Comparison of unconfined compressive strength profiles of the San Ysidro and TTR penetration sites with the Los Lunas site.

REFERENCES

1. S. W. Butters, H. S. Swolfs, J. N. Johnson, D. K. Butler, and P. F. Hadala; "Field, Laboratory and Modeling Studies on Mount Helen Welded Tuff for Earth Penetration Test Evaluation"; Terra Tek, Inc.; TR 75-9; August 1976.

2. W. J. Patterson; Letters to Defense Nuclear Agency and Waterways Experiment Station dated 28 July 1975, 8 September 1975, 18 June 1975, and 26 August 1975; Sandia Laboratories, Albuquerque, NM.

3. D. K. Butler, R. R. Nielsen, R. R. Dropek, and S. W. Butters; "Constitutive Property Investigations in Support of Full-Scale Penetration Tests in Dakota Sandstone, San Ysidro, New Mexico"; Technical Report S-77-3; April 1976; U. S. Army Engineer Waterways Experiment Station, CE, Vicksburg, MS.

4. L. A. Woodward; "Siltstone Sites for Penetration Tests, New Mexico"; Letter report to U. S. Army Engineer Waterways Experiment Station, September 1975; University of New Mexico, Albuquerque, NM.

5. J. Q. Ehrgott and R. C. Sloan; "Development of a Dynamic High-Pressure Triaxial Test Device"; Technical Report S-71-15; November 1971; U. S. Army Engineer Waterways Experiment Station, CE, Vicksburg, MS.

6. R. A. Knott; "Effect of Loading Rate on the Stress-Strain Characteristics of a Clay Shale in Unconsolidated-Undrained Triaxial Compression"; Miscellaneous Paper S-73-68; December 1973; U. S. Army Engineer Waterways Experiment Station, CE, Vicksburg, MS.

7. P. F. Hadala; Letter to W. M. Patterson: Sandia Laboratories, Albuquerque, NM; 30 September 1976; U. S. Army Engineer Waterways Experiment Station, CE, Vicksburg, MS.

DISTRIBUTION LIST

Address	No. of Copies
Director, Defense Nuclear Agency, Washington, D. C. 20305	
ATTN: STSI (Archives)	1
STTL (Technical Library)	2
SPSS	5
DDST	1
Sandia Laboratories, P. O. Box 5800, Albuquerque, New Mexico 87115	
ATTN: Doc Control for William Patterson	1
Doc Control for C. Wayne Young	1
Doc Control for 3141 Sandia Rpt Coll	1
Director, U. S. Army Engineer Waterways Experiment Station P. O. Box 631, Vicksburg, Mississippi 39180	
ATTN: Mr. D. K. Butler	1
Dr. P. F. Hadala	1
Dr. J. G. Jackson, Jr.	1
Library	3
Terra Tek, Inc., University Research Park, 420 Wakara Way Salt Lake City, Utah 84108	
ATTN: Mr. S. J. Green	1
Mr. S. W. Butters	1
Technical Library	1
Defense Documentation Center, Cameron Station, Alexandria, Virginia 22314	
ATTN: TC/Mr. Myer B. Kahn	2
HQDA (DAEN-ASI-L) Washington, D. C. 20314	2
HQDA (DAEN-RDL) Washington, D. C. 20314	1